INTERANNUAL VARIABILITY IN RADIATIVE FORCING BY DESERT DUST IN SNOWCOVER IN THE COLORADO RIVER BASIN

by

S. McKenzie Skiles

A thesis submitted to the faculty of
The University of Utah
in partial fulfillment of the requirements for the degree of

Master of Science

Department of Geography

The University of Utah

August 2010

The University of Utah Graduate School

STATEMENT OF THESIS APPROVAL

The thesis of **S. McKenzie Skiles**

has been approved by the following supervisory committee members:

Thomas H. Painter	, Chair	**05/26/2010**
Richard R. Forster	, Member	**05/26/2010**
S. Deems	, Member	**05/26/2010**

and by [redacted]

the Department of [redacted]

and by Charles A. Wight, Dean of The Graduate School.

ABSTRACT

Dust in snow accelerates snowmelt through its direct reduction of snow albedo and its further indirect reduction of albedo by accelerating the growth of snow effective grain size. Since the Anglo expansion into the western United States that began in the mid 19th century, the mountain snow cover of the Colorado River Basin has been subject to five-fold greater dust loading, largely from the Colorado Plateau and Great Basin. Previous work showed that in 2005 and 2006, dust loading in the San Juan Mountains (east central CRB) caused springtime surface radiative forcing of 25 to 50 W/m^2 and shortened snow cover by 25 to 35 days. This research will expand on prior work by assessing the interannual variability in radiative forcing, melt rates, and shortening of snow cover duration from 2005 to 2009, and the relative response of melt rates to simulated increases in air temperature. The number of recorded dust deposition events has increased monotonically since 2005, but the greatest dust loadings by mass occurred in 2006 and 2009. The dust loading in 2009 was a factor of 5 greater than 2006, and an order of magnitude greater than the other years in this time series. In 2009, snow albedo was less than 0.35 for the last 3 weeks of snow cover whereas in previous years albedo was rarely less than 0.50. With continued soil disturbance and projected drought in the southwestern US under global warming scenarios, the 2009 season may represent a new regime of dust forcing of radiative and hydrologic systems in the intermountain west.

TABLE OF CONTENTS

LIST OF FIGURES

LIST OF TABLES

CHAPTER 1

LITERATURE REVIEW

Introduction

Snow covered glaciers and seasonal snow cover supply 1/6th of the world's population with water (Barnett et al., 2005). In the western United States, the mountain snowpack provides roughly 75% of the water to over 60 million people who depend directly on mountain river basins and/or their associated reservoirs and aquifers for their water resources (Bales et al., 2006). In addition to water use by human populations, peak runoff typically coincides with increasing solar irradiance in the spring allowing for optimal conditions for plant growth, which influences plant phenology in mountain environments and downstream (Steltzer et al., 2009).

Snow cover also plays an important role in the Earth's surface energy budget through its high albedo and low thermal conductivity (Lemke et al., 2007). Over 15% of the earth's surface are covered by snow and ice annually, and due to snow's high reflectivity it contributes to the global energy balance by reflecting up to 90% of incoming solar radiation (Lemke et al., 2007). When snow cover extent is reduced a positive feedback cycle further reduces snow extent by exposing more land, which absorbs more solar irradiance, increases ground temperatures, and results in further reduction of snow extent.

Some studies show that changing climate has impacted snow cover and the hydrologic cycle, through reduced snow water equivalent and earlier runoff (Barnett et al., 2005; Mote, 2003; Stewart et al., 2004). According to the 2007 IPCC synthesis report, warming of the climate is unequivocally evident from observations of increases in global average air and ocean temperatures, widespread melting of snow and ice, and rising global sea level (IPCC, 2007a). When temperatures in winter and spring increase, the result in some mountain environments is more precipitation falling as rain, increased winter runoff, reduced water stored as snow, earlier peak runoff, and reduced summer streamflow (Dettinger et al., 2004; Leung et al., 2004; Mote, 2003). These trends, while influenced by interannual and decadal-scale climate variability, are being influenced by temperature trends that are consistent with observations of global warming over the 20th century (Hamlet et al., 2005). Barnett et al. (2008) demonstrated statistically that the majority of the observed low frequency changes in the hydrological cycle such as river flow, temperature, and snowpack, over the western US from 1950 to 1999, are due to human-induced climate changes from greenhouse gases and aerosols.

Other studies show changes in snowmelt and the hydrologic cycle, such as earlier spring runoff, are being impacted by aerosol deposition on snow (Painter et al., 2007; Qian et al., 2009) It is well known that impurities on the snow's surface increase the amount of absorbed solar radiation (Bohren and Huffman, 1998; Conway et al., 1996; Warren and Wiscombe, 1980). Impacts of black carbon on snow cover have been studied and modeled (Flanner et al., 2009; Flanner et al., 2007; Hansen and Nazarenko, 2004; Qian et al., 2009) and the 2007 IPCC report listed radiative forcing induced by soot on snow as one of the most important anthropogenic forcing mechanisms affecting climate

change between 1750 and 2005 (IPCC, 2007a). The role that dust plays in radiative forcing of snow has only recently been studied due to the lack of availability of detailed radiation and snow energy balance measurements (Painter et al., 2007).

Changes in runoff and potential water shortages would strongly impact the Colorado River Basin (CRB), which drains parts of seven states and Mexico and provides water supply, flood control, and hydropower to a large area of the southwestern US. Much of the CRB is arid and the water resources are dependent on melt water from high elevation snow pack, making them sensitive to snow accumulation and melt processes (Christensen and Lettenmaier, 2007; Christensen et al., 2004). The Colorado River has the highest fraction of allocated flow of any river in the world, due in part to its apportionment in 1922 in the Colorado River Compact between the Upper and Lower Basins and Mexico, based on discharge of a period of abnormally high flow (Christensen et al., 2004). Currently this system demands only slightly less then the long-term mean annual inflow (Barnett and Pierce, 2009). Due to the reliance of the Colorado River on snowmelt, it is of great interest to better understand the energy fluxes that cause snowmelt in the CRB and the relative capacity of a warming climate and deposited desert dust to influence these fluxes.

Previous Work

Painter et al. (2007) showed that the acceleration of melt by the shortwave radiative forcing of dust results in a shortening of snow cover duration in southwest Colorado on the order of 1 month. This study used detailed radiation measurements from the Senator Beck Basin Study Area of the San Juan Mountains, CO to determine the relative contributions of changes in dust concentration and grain size to changes in snow

albedo. From this partitioning, Painter et al. (2007) estimated the radiative forcing of dust in snow and in turn modeled the evolution of snow cover and its melt in the absence of dust.

This degree of acceleration of snowmelt by dust is a relatively new factor in the western US. Neff et al. (2008) used proxy records of dust deposition from high-elevation lakes in the same study area, which is located downwind of major western deserts, to infer accumulation rate and geochemical properties of lake sediments for the past 5,000 years. They found that dust load levels increased by 500% above the late Holocene average following increased settlement of the western United States during the 19th century. The larger dust flux persisted into the early 21st century; a slight decline in the mass accumulation rate was seen around the enactment of the Taylor Grazing Act of 1934. This act imposed regulations that restricted grazing activities on public lands, which strongly suggests that increased accumulation rates can be attributed to disturbance of dryland soil surfaces in the western United States, especially disturbance by grazing (Neff et al., 2005).

Dust Disturbance and Deposition

There is potential for dust deposition onto snow cover in many of the world's mountain ranges during the late winter-spring when dust storm activity peaks due to unstable atmospheric conditions (Kaspari et al., 2009). To better understand the processes of dust deposition into mountain snow cover it is important to understand the conditions under which it occurs.

There has been some study into dust disturbance, meteorological conditions, and subsequent deposition in snow cover (Franzén et al., 1994; Schwikowski et al., 1995;

Thompson et al., 2000; Wake and Mayewski, 1994). These studies have found that snow cover containing dust is downwind from large arid or semiarid environments, which have often undergone disturbance. In arid environments there is less organic matter and vegetative cover to provide soil surface protection (Belnap and Gillette, 1998), and sediment is produced from soil surface when wind forces exceed soil threshold frictional velocities (TFV's). Disturbance can enhance erosion by reducing TFV's (Belnap and Gillette, 1998). The eroded sediment can become entrained and deposited downwind.

Studies in the European Alps have shown that there is desert dust deposition into the snowcover, that the dust is far-travelled, and that predominant wind patterns influence dust deposition on both intraannual and interannual time scales. De Angelis and Gaudichet (1991) used ice cores from the Mont Blanc summit area in the French Alps to study continental dust flux between 1955 and 1985 and attributed the predominant dust source to northern Africa. This study found that deposition events and flux exhibited temporal variability, with frequency of events increasing in April, and an increase in total flux since the early 1970s, with very high inputs occurring after 1980. Schwikowski et al. (1995) also found characteristically Saharan dust during the study of a single dust event at a high alpine site in Switzerland using cloud scavenging, mineralogical analysis, and back trajectories.

Deposition of desert dust has also been found and studied in central Asia. Kaspari et al. (2009) analyzed highly resolved ice cores spanning from 1650 to 2002 from the Everest region and found that rock and soil dust from arid regions of Southwest Asia, Arabian Peninsula, and Northern Sahara were the dominant source of trace elements transported to Mount Everest. Seasonal variability was exhibited with concentrations

peaking during the winter and spring due to high winds from dominant Westerlies and more turbulent atmospheric circulation. This finding is consistent with the observations of Wake and Mayewski (1994), which studied dust on snow deposition over a larger spatial scale in central Asia. Kaspari et al. (2009) found that factors such as soil moisture and temperature impacted dust generation at the surface, and the long-range transport appeared to be sensitive to particular atmospheric conditions. Interannual variability in dust loading was also found, with an increase in the number of periods of high dust concentration since 1800. The timing of this increase in dust concentration could indicate the potential for anthropogenic influence but this study could not conclusively attribute the increase to anthropogenic inputs.

Thompson et al. (2000) studied a glacier ice core from the Himalaya (Dasuopu) and found increased dust deposition during an intense drought between 1790 and 1796; and a four-fold increase in deposition was recorded during the 20th century. The recent increase in total dust concentrations was attributed to increased anthropogenic activity in India and Nepal. Interannual variability in flux was also found, which was attributed to changes in meteorological conditions.

Additional studies have analyzed dust flux from South America over the Antarctic Peninsula (McConnell et al., 2007; Pereira et al., 2004). While this deposition is not occurring in alpine environments these studies are useful due to their analysis of long-term trends in interrannual variability of dust transport. Periera et al. (2004) looked at the airborne particulates in the atmosphere of Chilean Patagonia and compared them to particulates in an ice core from the Antarctic Peninsula. They found a high similarity between particles in the Patagonia atmosphere and the snow and ice from the peninsula,

with dust and anthropogenic particles peaking from November through March (austral summer). McConnell et al. (2007) used an ice core from the Antarctic Peninsula with a temporal record from 1832-1991, and found that dust concentrations varied interannually. They also found a doubling of dust levels during the 20th century, which was attributed to increased dust mobility and export due to land-use changes such as overgrazing and deforestation which, coupled with a warming climate, is leading to desertification in southern South America (McConnell et al., 2007).

Disturbance of vulnerable soils in semiarid and arid regions of the western US can lead to deposition into nearby alpine environments (Belnap and Gillette, 1998; Neff et al., 2005; Painter et al., 2007). The areas that are responsible for the majority of emissions in North America are Great Basin, Colorado Plateau, Mojave, and Sonoran deserts of the southwestern US (Neff et al., 2008). These areas have experienced widespread land-use change over the past two centuries with increases in grazing and agricultural activities that most likely increased soil vulnerability to wind erosion from these regions (Neff et al., 2005). The possibility of human-induced changes in atmospheric dust deposition was investigated by Neff et al. (2008) with use of proxy records from high elevation lakes in the San Juan Mountains in southwestern Colorado. Results indicate that increased sedimentation corresponds to settlement of the west; sediment accumulation rate over the past 150 years are more than five times greater than the average accumulations rate over the past 5,000 years (Neff et al., 2008).

Additional areas are being impacted by increases in dust emission and deposition beyond the areas discussed. Dust emission events have increased in China from the Takliman and Gobi deserts, which can deposit sediments in the Tien Shan and Altai

Ranges (Liu and Diamond, 2005). The Tien Shan, Altai, Pamir, and Himalaya are also being impacted by increased dust emissions from the drying of the Aral Sea (Waltham and Sholji, 2002). Alpine environments in Central Asia, Europe, and western US are likely to continue seeing these patterns, which may intensify with a changing climate and increasing drought conditions in the Middle East, Sahel, and southwestern US (Cook et al., 2004; Hansen et al., 2005; IPCC, 2007b). In addition to a changing climate, increasing populations and subsequent land use changes such as expansion of agriculture and grazing into arid and semiarid lands could lead to desertification and disturbance of soils which would drive increasing frequency and magnitude of dust emission events (Asner, 2005).

The studies discussed in this section address temporally variable dust flux and concentrations, the conditions under which they occur, and source regions. They do not address the radiative impacts of dust in snow; Painter et al. (2007) showed that dust in snow could shorten snow cover duration by up to 1 month. This study is intended to enhance the current understanding of impacts from dust in snow in alpine environments by further investigating radiative impacts through analysis of interannual variability in dust deposition and radiative forcing.

Snow Melt and Snow Energy Balance

In order to understand how radiative forcing by dust in snow impacts snowmelt hydrology, it is important to understand the energy fluxes that influence snowmelt. Energy inputs and exchanges at the snow's surface, within snow cover, and at the ground-snow interface are described by the snow energy balance equation, which can be expressed as:

(1) $$\frac{dU}{dt} + Q_m = (1-\alpha)S + L^* + Q_s + Q_v + Q_g$$

where

$\frac{dU}{dt}$ is change in internal energy over time, Q_m is energy available for melt, α is albedo so that 1 - α describes the fraction of absorbed solar radiation (S) at the snow surface, L^* is net longwave radiation, Q_s is sensible heating flux, Q_v is latent heat flux, Q_g is ground heat flux. The left side of the equation represents the response of the snowpack, whereas the right side represents the energy fluxes influencing the snowpack. The snow pack is cooling when $\frac{dU}{dt}$ is negative and the right side of the equation is negative. The snow is warming but not melting when snow temperature $T_s < 0$ ^oC and $\frac{dU}{dt}$ is positive, and then melt is initiated when $T_s = 0C$, $\frac{dU}{dt}$ is 0, and Q_m is positive. Snow cannot be warmer than 0 ^oC; melt occurs when the majority of the snowpack reaches 0 ^oC (Marks et al., 1998).

Energy for snowmelt comes primarily from absorbed solar radiation, which is controlled by albedo (Marks et al., 1998). Freshly fallen snow has the highest albedo of any naturally occurring surface, as high as 0.9 (broadband). This indicates that it is reflecting ~90% of incoming broadband solar radiation and absorbing ~10%. The albedo for visible wavelengths can be even higher, from 0.95- 0.98. This characteristic of snow

cover can drastically change the energy balance over a given landscape. For example, snow cover can change the albedo of grassland by a factor of three to four and forested regions by a factor of two to three (Betts and Ball, 1997; Thomas and Rowntree, 1992).

Most literature cites that snow albedo can range from 0.4-0.9: this is controlled by snow optical grain size and impurity content, with snow impurities having the greater impact (Conway et al., 1996). Grain size increases over time and with increasing temperature, which acts to decrease snow albedo. Freshly fallen snow is the most efficient reflector due its small grain size and greater scattering potential. Older snow has a lower albedo than freshly fallen snow due to the reduction of snow surface area to volume ratio (or specific surface area) through snow metamorphism. In general, the process of metamorphism increases snow density and increases the absorbing path length for photons by increasing grain size.

Deposition and scavenging of aerosols, such as soot and dust, into snow decreases albedo because aerosols are more absorptive than the ice particles that make up snow (Warren and Wiscombe, 1980). The dust or soot particles are heated by absorbing solar radiation and in turn heat the surrounding snow through conduction. Persistence at the snow surface and timing of deposition determines the influence of impurities on snowmelt.

Persistence at the snow surface influences radiative forcing because impurities in snow impact melt up to 30 cm below the surface, depending on the density, due to light being scattered between snow grains. There are different kinds of impurities and each impacts the snow in different ways. Black carbon particles are very efficient absorbers due to their large absorption coefficient and can have a significant impact on radiative

forcing, but are hydrophobic and do not stay at the snow surface for a substantial amount of time, especially in the spring when there is liquid water present in the snowpack (Conway et al., 1996; Qian et al., 2009). Black carbon particles can persist at the surface if they mix internally or externally with other hydrophilic aerosols such as dust (Qian et al., 2009). While dust is usually less absorptive than soot, it may have a larger impact in seasonal snow cover because of its higher concentrations and persistence at the snow surface throughout the melt season.

Timing of impurity deposition has an influence on radiative forcing; the largest impact being in the spring when solar irradiance is increasing. Dust that is deposited in winter is usually buried by additional snow accumulation, limiting the amount of time it is absorbing solar radiation at the snow surface. In the spring when solar irradiance increases and the internal energy in the pack is great enough to initiate snowmelt, dust layers persist at the surface and multiple layers can converge to enhance snowmelt. Often spring dust events bring additional dust deposition, which further accelerates snowmelt through its direct reduction of albedo**,** and its further reduction of albedo by accelerating the growth of snow grains (Painter et al., 2007).

Measuring snow energy balance and snowmelt requires detailed monitoring of surface climate, which can be difficult in high elevation variable terrain (Marks et al., 1992). While detailed snow energy balance measurements are limited in alpine environments a few sites have been established for these measurements (Marks et al., 1992; Painter et al., 2007).

Marks and Dozier (1992) presented a detailed evaluation of alpine surface climate, energy exchange, and snowmelt using measurements from a study site in the

Sierra Nevada for the 1986 water year to approximate snow cover energy balance. A combination of meteorological measurements and model parameters were used to calculate the net energy transfer to the snow cover by solar and thermal radiation, sensible and latent heat exchange with the atmosphere, conduction from the soil, and advected heat transfer from precipitation. The study evaluated the magnitude and relative importance of each form of energy transfer. This was done to determine which of these measured parameters was most critical and what type of simplifying assumptions could be used in snowmelt calculations. During the 1986 water year, Marks and Dozier (1992) found that net radiation contributed the largest amount of energy for snowmelt, 5 to 10 times the energy for melt over the combination of all other fluxes. The next largest energy contribution was sensible and latent heating, and soil conduction and advection provided negligible energy for snowmelt. The study also showed that the calculations of energy flux were reliable during melting conditions, because calculations of snowmelt based on summing the totals of each energy transfer term resulted in mass balance which was very close to the measured precipitation input, and to measured discharge from the watershed during the same period of time (Marks and Dozier, 1992).

Research into the physical processes that control snowmelt in alpine environments has led to the development of both explanatory and predictive models. The study by Marks and Dozier (1992) was used to validate the snow energy balance snowmelt model, SNOBAL, which was presented in Marks (1988) and explained in further detail in Marks et al. (1998) and is used in the present study. SNOBAL is a two-layer model, which uses point measurements of energy balance forcing variables to calculate snowpack energy and mass balance to simulate the accumulation and ablation of seasonal snow cover.

Temperature Change

In addition to the impacts from dust in snow there are also changes in hydrologic cycle in the western United States that are attributable to climate change (Pierce et al., 2008). The Intergovernmental Panel on Climate Change (IPCC) 2007 synthesis report states that warming of the climate system is unequivocal and is evidenced by observations of increases in average air and ocean temperatures, widespread melting of snow and ice and rising global average sea level (IPCC, 2007a). Climate change is defined by the IPCC as change in the state of the climate that can be identified by changes in the mean and/or the variability of its properties, and that persists for an extended period, typically decades or longer, and refers to any change in climate over time, whether due to natural variability or as a result of human activity.

Climate change occurs when factors alter the energy balance of the climate system. These factors include changes in land cover, solar radiation, and atmospheric levels of greenhouse gases and aerosols, which impact the absorption, scattering, and emission of radiation with the atmosphere and at the earth's surface. These changes in energy are the drivers of climate change, can be positive or negative, and are expressed as radiative forcings (W/m^2), where radiative forcing is defined as a change in net irradiance at the tropopause after allowing for stratospheric temperatures to readjust to radiative equilibrium, but with surface and tropospheric temperatures and state held fixed at the unperturbed values (IPCC, 2007a).

While climate change may be driven by both natural and anthropogenic causes, the observed increases in global average temperatures since the mid-20^{th} century is very likely due to the increase in anthropogenic green house gas (GHG) concentrations (IPCC,

2007a). The global average effect of human activity since 1750 has been one of warming, with a radiative forcing of +1.6 W/m^2, which is very close to +1.66 W/m^2, the value attributed to GHG's since 1970 (IPCC, 2007a).

The 2007 IPCC report states with high confidence that many semi arid regions will suffer a decrease in water resources due to climate change. This decrease will exacerbate current stresses on water resources from population growth, economic, and land use change. The impact of which will be noticed most strongly in regions that depend on melt from mountain snowpack for freshwater like the western United States (Leung et al., 2004).

Observational studies have documented a decline in snowpack across much the western US over the period 1950-99 (Groisman et al., 1994; Groisman et al., 2004; Mote, 2003; Mote et al., 2005). Groisman et al. (1994) found a statistically significant reduction in snow cover extent over North America using remote sensing imagery. Groisman et al. (2004) used National Weather Service Cooperative network station data to show March snow cover extent in the western US has diminished since 1950. Using data from snow courses Mote (2003) and then Mote et al. (2005) showed a reduction in 1 April snow water equivalent (SWE) between 1950 and 2003 over the western United States, with the exception of the southern Sierra Nevada. These observed reductions in snowpack could be explained in part by that between 1949 and 2004 there has been a regional trend toward more winter precipitation falling as rain instead of snow (Knowles et al., 2006).

These studies rely on observations, and while observed data provides direct empirical evidence of trends over the western US there are problems with limited spatial coverage, coarse spatial resolution, and a relatively short time period of observations

(Hamlet and Lettenmaier, 2005). Observations from snow course measurement have had a reasonably consistent level of coverage over the western US for the period from about 1950 to present, which constrains the period of record to about half a century. This short time period according to Hamlet et al. (2005) makes attributing observed SWE losses to long-term climate change difficult because the record has been shown to contain trends in precipitation and temperature that are strongly influenced by interannual and decadal-scale climatic variability associated with the El Niño-Southern Oscillation (ENSO) and the Pacific decadal oscillation (PDO) (Hamlet et al. 2005).

Climate is a challenging system to simulate due to the number of interacting components and the wide range of time and spatial scales of relevant processes, but there have been studies that have attempted to decouple the natural variability of decadal scale influences from the anthropogenic influenced warming using modeling and statistical methods. Hamlet et al. (2005) used the Variable Infiltration Capacity (VIC) hydrologic model to simulate April 1 SWE between 1915-2003, and separated the trends due to temperature and precipitation during different simulations. The study found that downward trends in 1 April SWE over the western US were not well explained by decadal climate variability but were shown to be primarily due to widespread warming. Mote et al. (2005) also found that internal climate variation, such as the Pacific Decadal Oscillation (PDO), was not enough to explain the magnitude of the observed warming and decrease in snow water equivalent. Pierce et al. (2008) investigated the relationship between warming and decreasing snow trends by using global climate and regional hydrologic models and multivariable detection and attribution methodology to

demonstrate statistically that the majority of the low-frequency changes in the hydrologic cycle are due to human caused climate changes from greenhouse gases and aerosols.

These previous studies made use of climate and hydrology models to investigate the relationship between observed warming and other observed trends. If these increasing temperatures trends continue over river basins with substantial snow accumulation, as predicted by climate change assessments, scenarios of increasing winter and spring temperature in climate change assessments typically result in increased winter runoff, reduced peak water equivalent stared as snow, earlier peak stream flows, and reduced summer stream flow (Hamlet et al., 2005).

Additional studies model the potential magnitude of future temperature increases, and in turn, the hydrologic impacts of these increases. Leung et al. (2004) modeled potential temperature increases by use of dynamical downscaling of ensemble GCM's of present and future climate over the western US, and showed temperature increases of 1^{o}C-2.4^{o}C by midcentury. Christensen and Lettenmaier (2007) used two climate emission scenarios, IPCC SRES A2 (unconstrained GHG emission growth) and B1 (emissions capped by 2100) to run ensemble of 11 downscaled GCMs. Results from the A2 and B1 scenarios were compared to model outputs run with historical observations from 1950-1999. All the models agreed that temperatures would increase over time, with the mean temperature change over these time periods for the A2 emissions ranging from 1.2^{o}C to 4.4^{o}C and the B1 scenario from 1.3^{o}C to 2.7^{o}C.

While these studies are restricted to investigations to increases in temperature, temperature change is not the only factor influencing runoff timing in the western US. Painter et al. (2010) uses the VIC model to simulate runoff in the CRB given dust

radiative forcing and resultant changes in surface albedo. These changes induce earlier runoff and reduced runoff volume due to prolonged evapotranspiration. The impacts from dust and increasing temperatures are largely independent, but are occurring at the same time. The relative capacity of these two factors to influence melt has not been investigated as of yet, which is another intent of this study.

CHAPTER 2

CURRENT STUDY AND RESEARCH QUESTIONS

Current Study

Desert dust deposition into the alpine snowpack of the Colorado River Basin can reduce snowcover albedo and advance snowmelt timing, which can cause changes in runoff intensity and timing. Due to the over-allocation and sensitivity of the Colorado River water resources to snowmelt runoff it is of interest to investigate the impact that dust is having on the hydrologic cycle in this region. Painter et al. (2007) showed that in 2005 and 2006 dust loading in the San Juan Mountains shortened snow cover by 18-35 days. In the present study we expand the previous work to encompass 2005 to 2009. While the number of dust events has increased monotonically since 2005, the greatest dust loading occurred in 2006 and 2009, with dust concentrations in 2009 being a factor of 5 greater than 2006 and an order of magnitude greater than the other years. Using a 5-year record of detailed energy balance measurements we can assess the interannual variability in radiative forcing, melt rates, and shortening of snow cover duration.

The Colorado River Basin and western United States is also being impacted by temperature change, which can impact snow duration and melt. We model longwave radiation under increased temperature scenarios to address the relative capacities of radiative forcing by dust and temperature increases to accelerate snowmelt.

Research Questions

Research questions are addressed through comparisons of measurements and modeling results. Measurements include dust concentrations collected at the study plots and snow energy balance measurements recorded at the instrumentation towers, from which radiative forcing is inferred.

This work addresses the following research questions:

1) How does radiative forcing by dust vary interannually in the Colorado River Basin?

This question is addressed through comparison of dust concentration measurements and estimated radiative forcings due to dust, over the five-year record. Radiative forcing in this case refers to the instantaneous enhanced surface absorption of solar radiation due to dust.

2) How are changes in melt out date and radiative forcing of dust in snow related at the seasonal scale?

This question is addressed through modeling snowmelt for observed conditions and a clean snowpack, which is the observed snowpack with radiative forcing due to dust removed. Modeled snowcover depletion and melt out date for these scenarios are then compared to end of year dust concentration.

3) What are the relative capacities of dust radiative forcing and temperature increase to accelerate snowmelt?

This question is addressed by modeling snowmelt under increased temperature scenarios, where temperature changes are used to model increases in longwave radiation. These temperature increases are applied and melt out compared under all scenarios;

observed conditions plus temperature increases and a modeled clean snowpack plus temperature increases.

CHAPTER 3

STUDY AREA AND METHODS

Study Area

The Center for Snow and Avalanche Studies (CSAS) operates two instrumentation towers in the Senator Beck Basin Study Area (SBBSA), established in 2002. SBBSA is in the Ouray Ranger District of the Uncompahgre National Forest in the western San Juan Mountains of southwestern Colorado. The study area is near US Hwy 550 at Red Mountain Pass. Figure 1 shows a map of the study area in relation to the Colorado River Basin.

Senator Beck Study Plot

Senator Beck Study Plot (SBSP), shown in Figure 2A, is located above treeline in the alpine tundra (3719 m), at a level site near the center of Senator Beck Basin Study Area. SBSP contains a 10 m tower holding the instrumentation array and a 12 m X 36 m snow profile plot. A hexagonal array of vertical 3 m snow depth measurement stakes are deployed around the tower at a radius of 7.5 m to calculate snow surface slope and aspect to improve the interpretation of reflected radiation being measured by the down-looking pyranometers and in turn the calculation of albedo. The site is exposed to alpine winds and measurements are considered representative of wind-affected snowcover formation.

Precipitation is not measured at SBSP due to high winds that would exacerbate undercatch. Wind speed and direction are measured at two heights, one at the top of the

SBSP tower to minimize the influence of the immediate terrain. Snowpack depth is measured at the end of each hour by an ultrasonic distance sensor. Air temperature and relative humidity are measured every 5 seconds at two fixed heights. Incoming and outgoing broadband solar and incoming longwave radiation values are measured every five seconds by individual sensors on the tower. Outgoing longwave radiation is inferred from measurement of snow surface temperature from infrared sensor. All subhour measurements are averaged each hour to generate hourly data, and every 24 hours to generate daily summary data. Measurements taken at the towers are summarized in Table 1.

Swamp Angel Study Plot

Swamp Angel Study Plot (SASP), shown in Figure 2B, is located in a clearing below treeline in a subalpine forest at 3368 m. It is a protected site that is an ideal location for measuring precipitation and snowpack accumulation. Wind speeds are very low and wind redistribution of snowcover is negligible. The snow profile plot is 30 m x 30 m and contains the stand-alone precipitation gauge and 6 m tower holding the instrumentation array. The site is generally level, but also contains snow depth stakes to calculate snow surface slope and aspect. The Senator Beck Stream Gauge (SBSG) is located just below SASP at the 'pour point' of the basin.

Precipitation (mm) is measured at SASP in an open topped collector; accumulated fluid is weighed every 5 seconds and reported hourly. The hourly data can be summed to daily totals and as a running total for the water year. Other measurements taken at the tower are identical to the measurements described for SBSP above, differing only in

tower height. All subhour measurements are averaged to generate hourly data and every 24 hours to generate daily summaries.

Measurements

Snowpack Measurements

Regular snow pits are used to monitor the evolution of the snowpack. The Center for Snow and Avalanche Studies profiles full column snow pits within the study plot boundaries by the met towers monthly during the winter, and then weekly during the ablation season; an example is shown in Figure 2C. Weekly sampling starts no later than April 15th, which is the average date of peak snow water equivalent, and begins earlier if significant dust deposition has occurred. Measurements in the snowpits include a temperature profile (every 10 cm), snowpack stratigraphy, liquid water content, and measurements of density within each layer. Using depth and density measurements, snow water equivalent (SWE) is calculated for each layer and the total snowpack. Other measurements include grain type and size, and observations of air temperature, wind, precipitation, and cloud cover are recorded each time a pit is dug. Dust stratigraphy is measured and quantified gravimetrically in the top 30 cm of the snow column at 3 cm intervals. Dust sampling is described further in the section below.

Dust Concentration Measurements

Sampling of dust layers begins when deposition events occur and concentrations are recorded per event and at the surface. Dust events are identified in the field by observers, and bulk samples (surface collections of dust concentrations) are collected per event for a 0.5 m^2 area. These samples are melted and sent to the Snow Optics Laboratory

where they are dried and preserved, and single event dust concentration is recorded. Subsets of these bulk samples are processed for texture and chemistry by the Earth Surface Processes Laboratory of the United States Geological Survey, CO.

Dust concentration in the top 30 cm of the snowpack, the approximate maximum depth at which dust can influence radiative forcing, are collected each time a snow pit is dug. Samples are taken at 3 cm vertical intervals for a total of 10 samples per collection; accurate sample volumes are maintained by use of a gravimetrics board, which is shown in Figure 2D. Each sample is filtered and weighed in the lab to find dust concentration. These two types of dust concentrations measurements, bulk and gravimetric samples, are used to address intra- and interannual variability in dust loading.

Energy Balance Measurements

In addition to the meteorological measurements described in the study area section above, measurements at the towers include incident and reflected fluxes for broadband shortwave and NIR/SWIR (from which the visible fluxes are calculated), longwave irradiance and snow surface temperature, and noontime diffuse irradiance. These measurements are used to address interannual variability in dust radiative forcing and as forcing variables for snowmelt modeling, described in more detail below.

Radiative Forcing

From the tower measurements, the range of potential radiative forcing due to dust is determined using the treatment described in Painter at al. (2007). Radiative forcing by dust in snow directly affects the snowpack through enhanced absorption by dust (first direct effect), indirectly through enhanced absorption by larger grain size due to

acceleration of grain growth from the first direct effect (first indirect effect), and enhanced absorption by the earlier exposure of a darker substrate (second indirect effect).

To account for the range of potential radiative forcing due to dust we calculate minimum and maximum radiative forcing. Minimum surface radiative forcing addresses the first direct effect of dust in snow by accounting for the reduction in visible albedo. The maximum radiative forcing addresses both the first direct effect as well as the first indirect effect by accounting for reduction in visible albedo due to dust and changes in grain size.

Minimum surface radiative forcing $F_{d\min}$ (W/m^2) is calculated as

(2) $$F_{d\min} = E_{vis}\Delta_{vis}$$

where

E_{VIS} is the visible irradiance (W/m^2) determined from the difference between the broadband and NIR/SWIR irradiances, $\Delta_{vis} = 0.92\text{-}\alpha_{vis}$, α_{vis} is calculated visible albedo and 0.92 is the mean visible albedo for dust event free snow.

Maximum surface radiative forcing $F_{d\max+i1}$ is calculated as:

(3) $$F_{d\max+i1} = 0.5(E_{vis}\Delta_{vis} + E_{NIR}\alpha_{NIR}((1/\xi)\text{-}1)$$

where

$$\xi = 1 - 1.689\Delta_{vis}; \quad \Delta_{vis} < 0.17$$

$$\xi = 0.67; \quad \Delta_{vis} > 0.17$$

E_{NIR} is the NIR/SWIR net shortwave flux, and α_{NIR} is the NIR/SWIR albedo. The latter relationship gives the proportion of the change in NIR/SWIR albedo due to the presence of dust versus grain coarsening in the absence of dust (Marks et al., 1998; Painter et al., 2007).

Snowmelt Modeling

Temperature Change

It is projected that the southwestern United States will become warmer and more arid over the next 50 to 100 years and downscaled global climate models project average temperature increases of 2 ^{o}C to 4 ^{o}C over the CRB (Barnett and Pierce, 2009). In this study the influence these increases in temperature have on snowmelt in the presence and absence of dust radiative forcing is assessed. The relative capacities of radiative forcing by dust and temperature increase to accelerate snowmelt is addressed by simulating snowmelt with increased temperature of 2 °C and 4 °C at every hour with dust and every hour without dust.

The increase in temperature influences sensible heating and longwave irradiance. The change in sensible heating is handled through the temperature increase whereas the increase in longwave irradiance is more complex to treat. The increase in longwave irradiance depends strongly on the fraction of sky that is cloud covered, a difficult variable to estimate. Therefore, the estimates of increases in longwave irradiance were bracketed with treatments for clear skies and cloudy skies.

Given air temperature and vapor pressure, clear sky longwave irradiance is modeled based on the parameterization described in Brutsaert (1975):

$$L = 0.642(e_a / T_a)^{1/7}(\sigma T_a^4) \quad (4)$$

where

L = longwave irradiance (W/m^2), e_a = vapor pressure (Pascals), T_a = air temperature (K), θ= Stefan-Boltzmann constant (5.67×10^{-8} W/m^2K^{-4}). This represents the Stefan-Boltzmann equation where $0.642(e_a/T_a)^{1/7}$ is the atmospheric emissivity.

Cloudy sky irradiance is modeled based on the parameterization described in Konzelmann et al. (1994) using air temperature, vapor pressure, and cloud cover fraction:

$$L = \{[0.23 + 0.483(e_a / T_a)^{1/8}](1 - n^3) + 0.963n^3\}\sigma T_a^4 \quad (5)$$

where

n= fractional cloud cover. In this case cloud cover is treated as complete, so *n*=1, for which the equation becomes, $L = (0.963)\sigma T_a^4$, where 0.963 is the apparent emissivity of the sky under complete cloud cover. T_a is then increased by + 2 °C and + 4 °C in both relationships to span the increase in longwave irradiance.

Snowmelt Model

We used the point snow energy balance snowmelt model, SNOBAL, to calculate snowmelt and predict point runoff using input data on snow properties, measurement

heights and depths, and energy exchanges. The model was first described conceptually by Marks et al. (1992) and then described in detail by Marks et al. (1998).

The snowpack is represented in the model by two layers, a 25 cm upper active layer and the remainder of the pack as a second layer. Melt is computed in either layer when the accumulated energy depletes the cold content. The cold contents are calculated using the following equation:

$$Q = \rho h c_s (T_0 - T^n) \tag{6}$$

where

ρ = snow density, h = snow height, c_s = specific heat of snow, T_0 = melting temperature, T^n = snow temperature.

The maximum liquid water holding capacity of the snow cover is a volume ratio defined as (Davis et al. 1985):

$$\frac{\text{volume of water}}{\text{volume of snow} / \text{volume of ice}} \tag{7}$$

The initial relative saturation of the snow cover is set as an initial condition. Runoff is estimated when the accumulated melt and liquid water content exceeds the liquid water capacity. Figure 3 is a conceptual diagram of the model taken from Marks et al. (1998).

The model is initialized with snowpack conditions collected weekly at each site as described above and is driven by hourly averages of net shortwave, incident longwave radiation, air temperature, relative humidity, and wind speed collected at the

instrumentation sites. In all cases the net shortwave used is estimated by taking the difference between the measurements at the tower of net broadband and NIR/SWIR radiation. The initial state variables are snow depth, snow density, surface layer temperature, total snowpack temperature, and snowpack liquid water content, these are updated hourly by the forcing variables. These are summarized in Table 2, taken from Marks et al. (1998). Figure 4 shows hourly averages of the measured and calculated parameters used as forcing variables: net shortwave, longwave irradiance, wind speed, vapor pressure, and air temperature for water years 2005-2009 at both sites. Due to data processing issues net solar radiation is plotted over the ablation season for 2005 and 2006 and then over the full water year for 2007-2009. Soil temperature is not plotted because its flux to the snowpack is considered to be a negligible energy contribution (Marks and Dozier, 1992) and is set to 0 for the model runs.

The model is used to predict snowmelt for all scenarios; observed conditions (‘dust case’), observed conditions with radiative forcings removed (min and max ‘clean case’), and each of these scenarios with the 2 °C and 4 °C temperature increases, which are summarized in Table 3. The equations used to estimate minimum and maximum radiative forcings due to dust are described in the radiative forcing section above.

Sensitivity and Uncertainty

While SNOBAL has been shown to reproduce measured conditions there is always some uncertainty in measurements and assumptions made in calculating energy flux in the model. Instruments and their ranges and accuracies are listed in Table 4. Uncertainty in measurements, and potential model sensitivity to each parameter, is

addressed by varying the values of the input parameters to the ranges in instrument accuracy at subalpine site (SASP) over the 2007 ablation season. Vapor pressure sensitivity is addressed by varying the RH accuracy range. Uncertainty and sensitivity for each parameter, individually and all parameters combined, is then assessed though comparison to model outputs for observed conditions.

The sensitivity of model runs to snow surface roughness, which is set as a constant 1 mm at the beginning of each model run, is also tested within this study. Some published roughness lengths for snow include 0.2 mm for fresh snow (Poggi, 1976), average of 1.9 mm for annual snow cover (Pluss and Mazzoni, 1994), and 1-12 mm for rough snow (Jackson and Carroll, 1978). Snow surface roughness is not constant and varies at different scales (Brock et al., 2006). The roughness of snow influences the movement of air across the snow surface, which in turn influences the transfer of energy through turbulent exchange. While dust in snow can have varying impacts on surface roughness, Fassnacht et al. (2009) found that dust in snow decreased the magnitude of roughness relative to adjacent clean snow surfaces by melting snow uniformly.

In this thesis, surface roughness was altered to 5 mm, 1 cm, and 5 cm to test the sensitivity of the model to this parameter. The sensitivity is assessed through comparison to model outputs run with the typical surface roughness height of 1 mm. The high value of 5 cm is used only to assess the model sensitivity, a surface roughness of 5 cm is unlikely, some of the highest surface roughness values recorded are 20-80 mm for very rough glacier ice (Smeets et al., 1999).

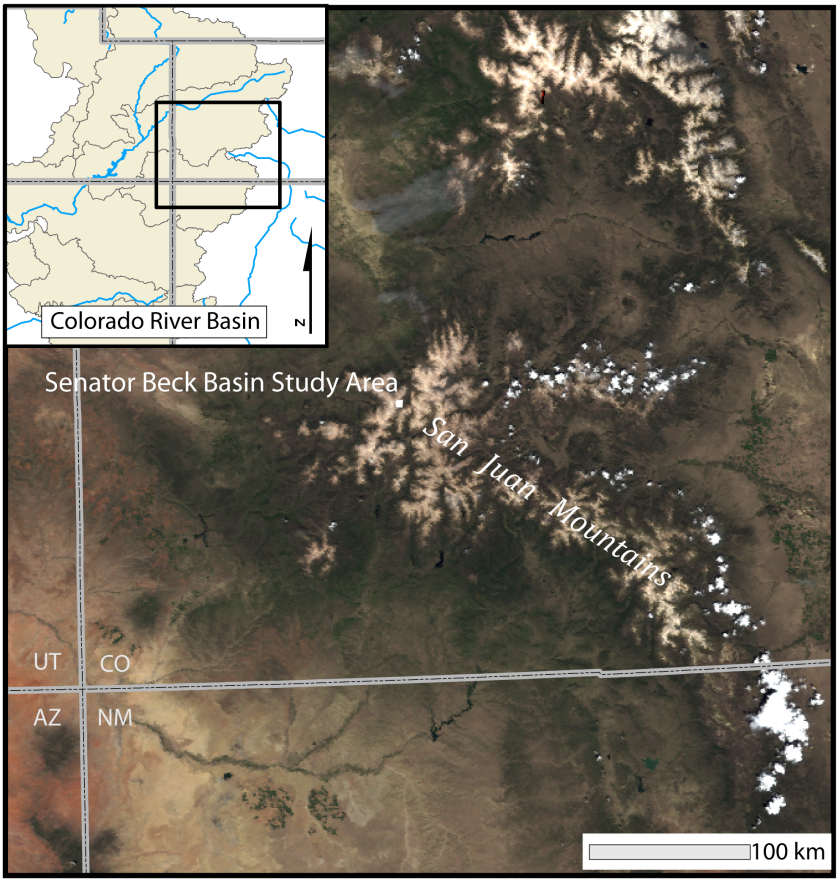

Figure 1 Map of Senator Beck Basin Study Area (SBBSA).

A.

B.

C.

D.

Figure 2 A. Met tower at Senator Beck Study Plot (SBSP) B. Met tower at Swamp Angel Study Plot (SASP) C. Snowpit to collect snowpack measurements within SASP boundaries D. Sampling dust concentration using gravimetrics board.

Table 1 Parameters measured at met towers.

Measured Parameters	SBSP (alpine)	SASP (subalpine)
Air temperature *	•	•
Relative Humidity *	•	•
Wind Speed *	•	•
Precipitation		•
Incident/Reflected Broadband Shortwave Radiation	•	•
Incident/Reflected NIR/SWIR Radiation	•	•
Longwave Irradiance	•	•

* at two heights

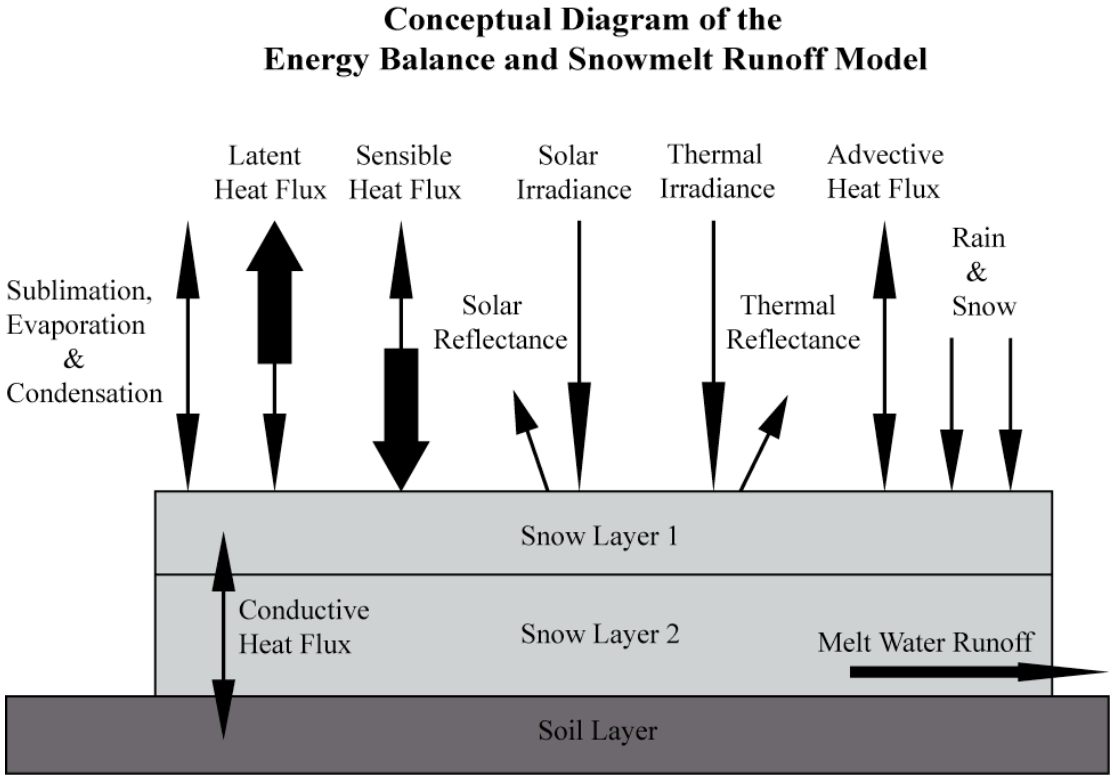

Figure 3 Conceptual diagram of SNOBAL adapted from Marks et al. 1998 with permission.

Table 2 SNOBAL state and forcing variables (Marks et al. 1998).

State Variables	Forcing Variables
Snow Depth (m)	Net Solar Radiation (W/m^2)
Snow Density (kg/m^3)	Incoming longwave radiation (W/m^2)
Snow Surface Layer Temperature (^oC)	Air Temperature (^oC)
Average Snow Cover Temperature (^oC)	Vapor Pressure (Pa)
Average Snow Liquid Water Content (%)	Wind Speed (m/s)

Table 3 Scenarios for which snowmelt is modeled using SNOBAL. Scenarios in bold are used as representative cases for presenting results. The 'Dust' scenario is the model output for the observed conditions, and the other representative cases are not actual model runs but calculated means of the preceding scenarios (i.e. the 'Clean' scenario is mean of the clean max and clean min model runs).

Scenarios							
Now		+2 °C Clear Skies	+2 °C Cloudy Skies		+ 4 °C Clear Skies	+ 4 °C Cloudy Skies	
Dust		Dust Clear +2	Dust Cloudy +2	*Dust +2*	Dust Clear +4	Dust Cloudy +4	*Dust +4*
Clean Max	*Clean*	Max Clear +2	Max Cloudy +2	*Clean +2*	Max Clear +4	Max Cloudy +4	*Clean +4*
Clean Min		Min Clear +2	Min Cloudy +2		Min Clear +4	Min Cloudy +4	

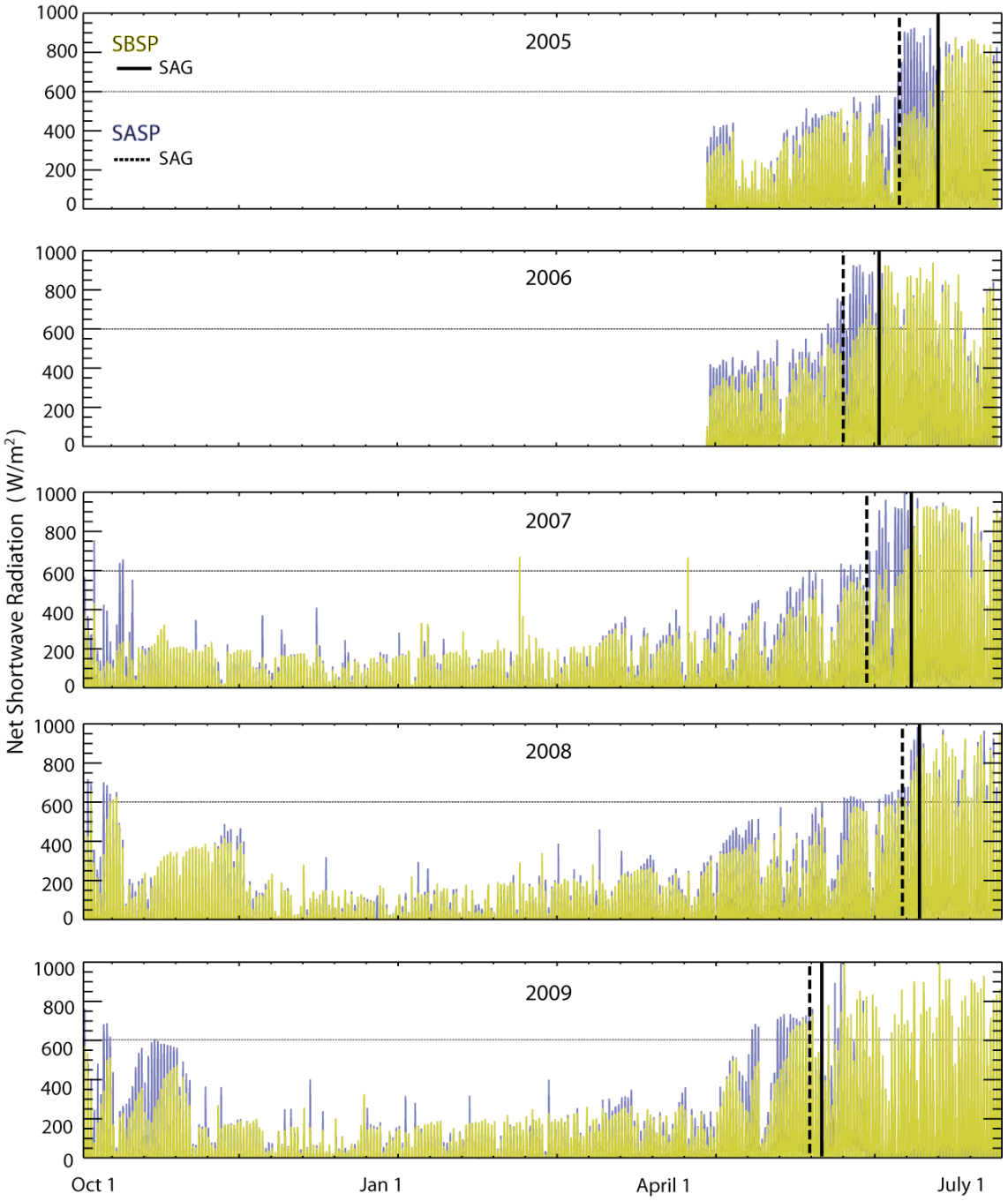

A.

Figure 4 Energy balance components plotted over the water year: shortwave radiation (A) is the difference of measurements of broadband and NIR/SWIR radiation; longwave irradiance (B) is measured by an pyrgeometer at the towers; air temperature (C) is the average of measured temperatures at two heights; vapor pressure (D) is calculated from measurements of air temperature and relative humidity; and wind speed (E) is the average of measurements at two heights.

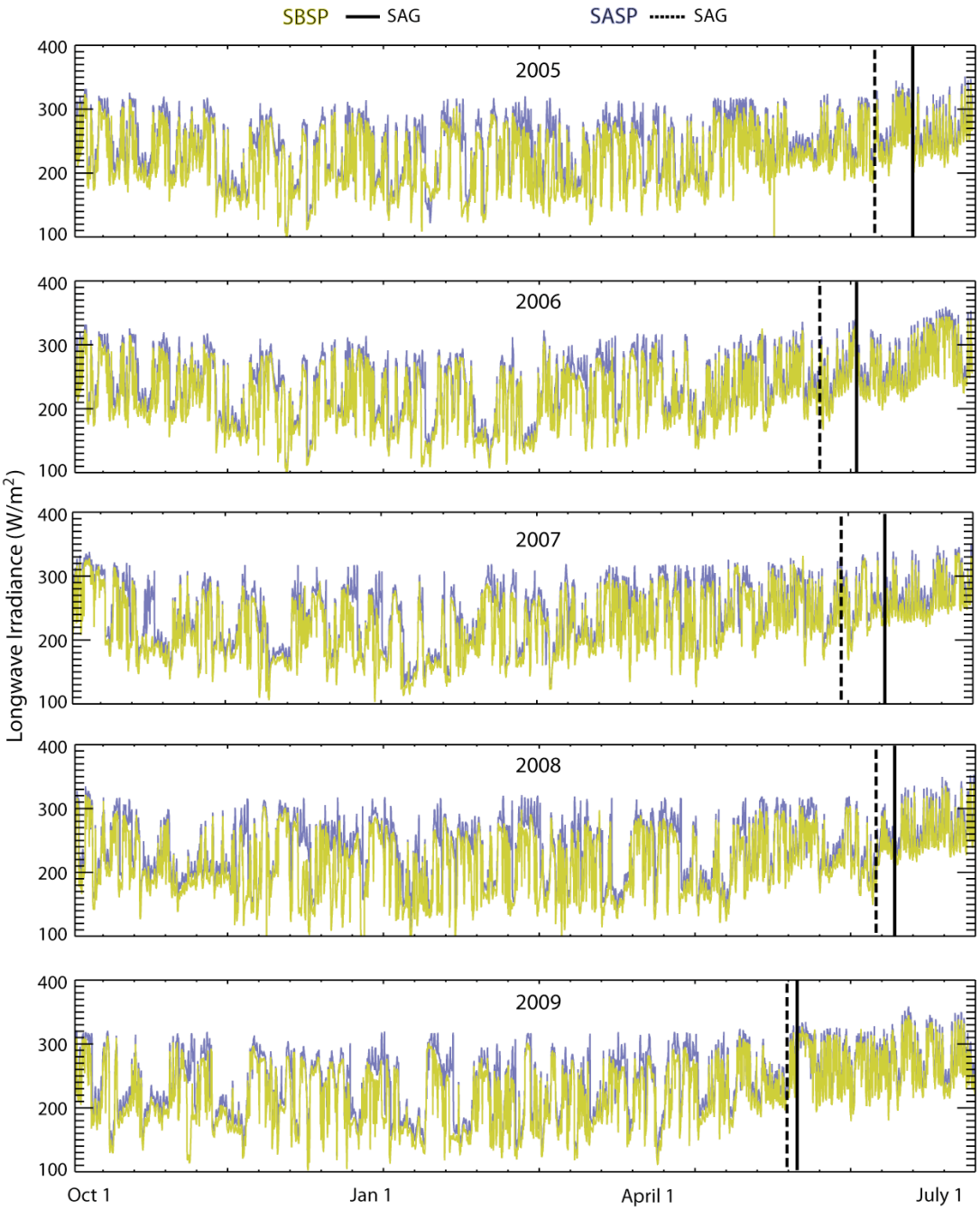

B.

Figure 4 continued.

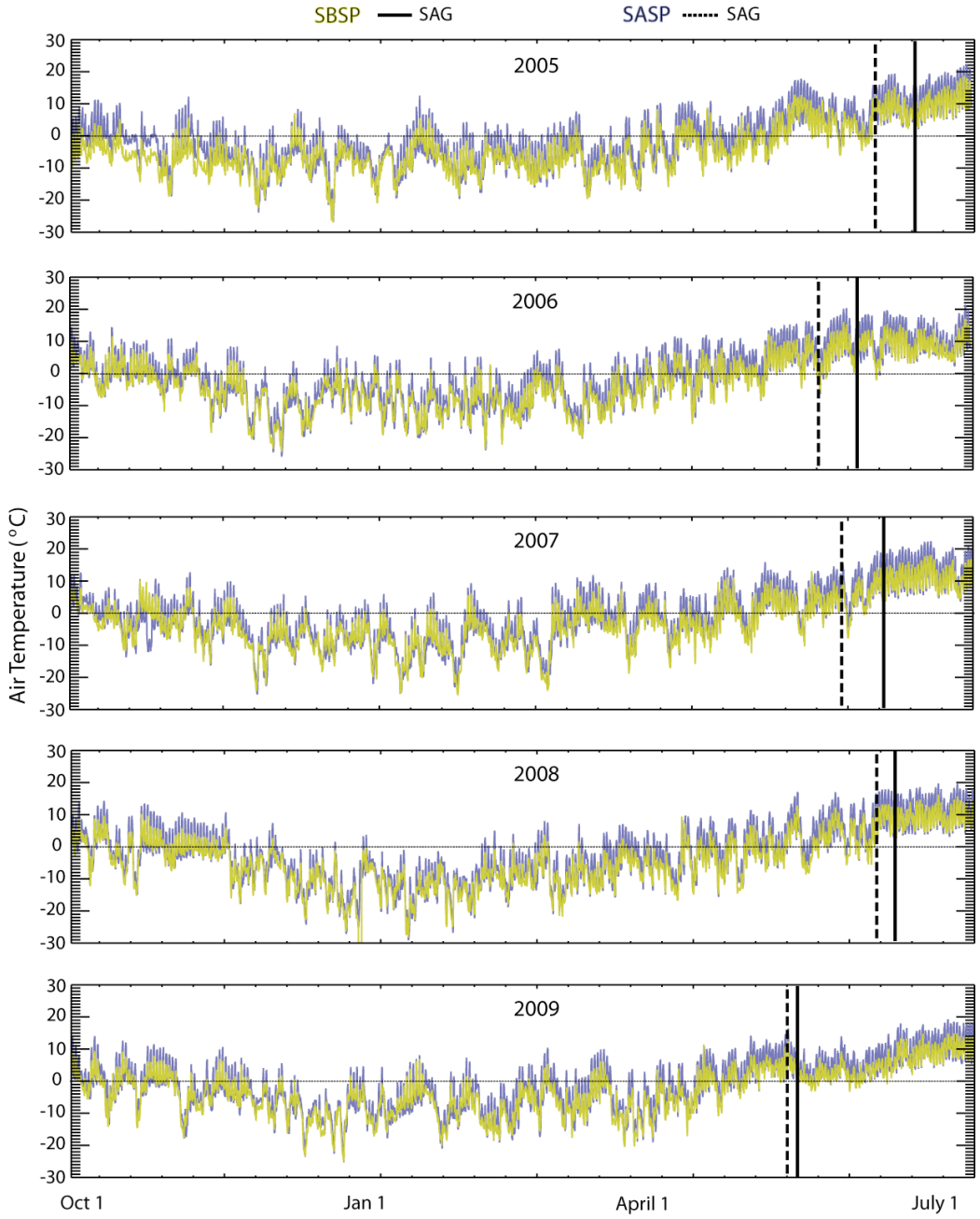

C.

Figure 4 continued.

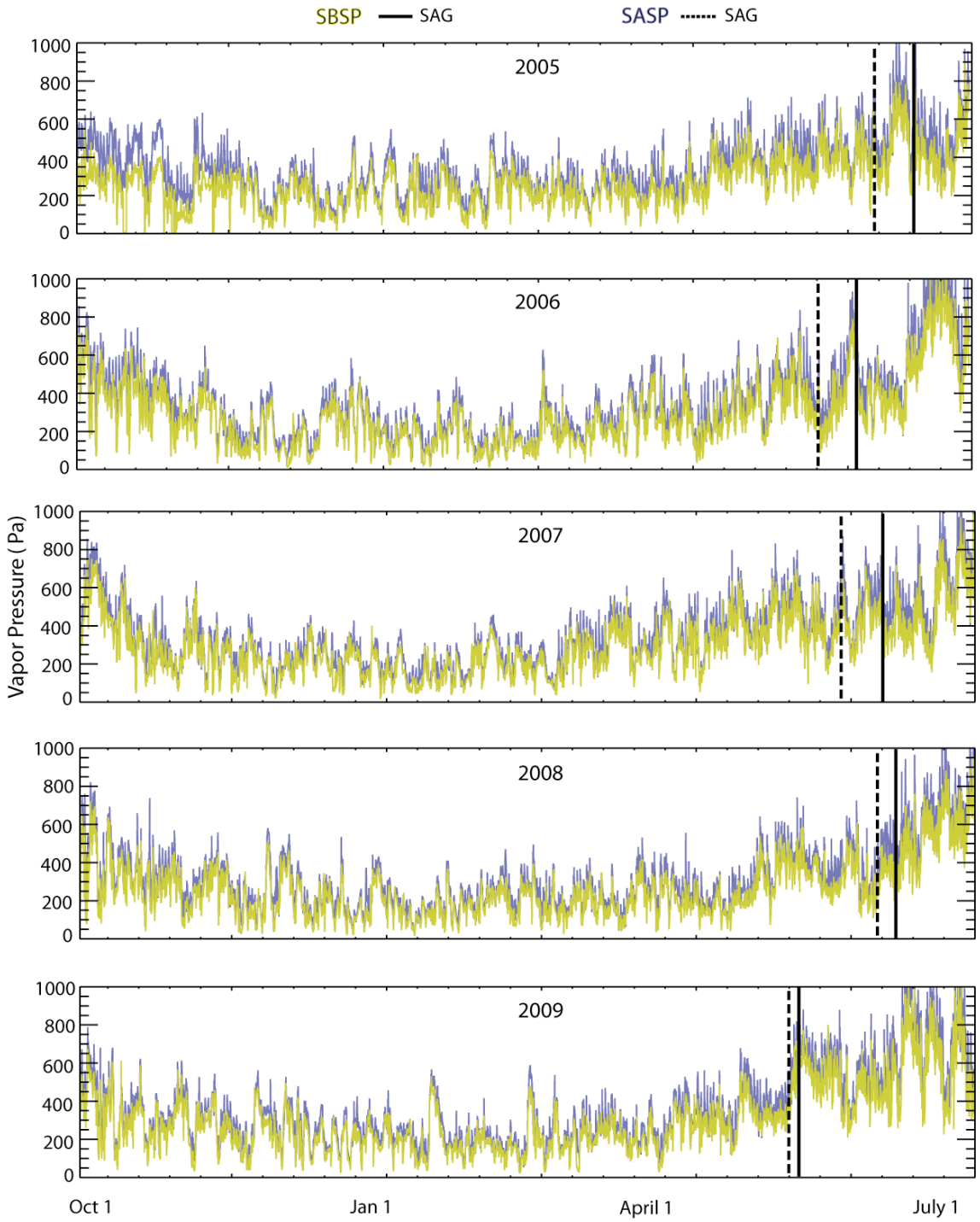

D.

Figure 4 continued.

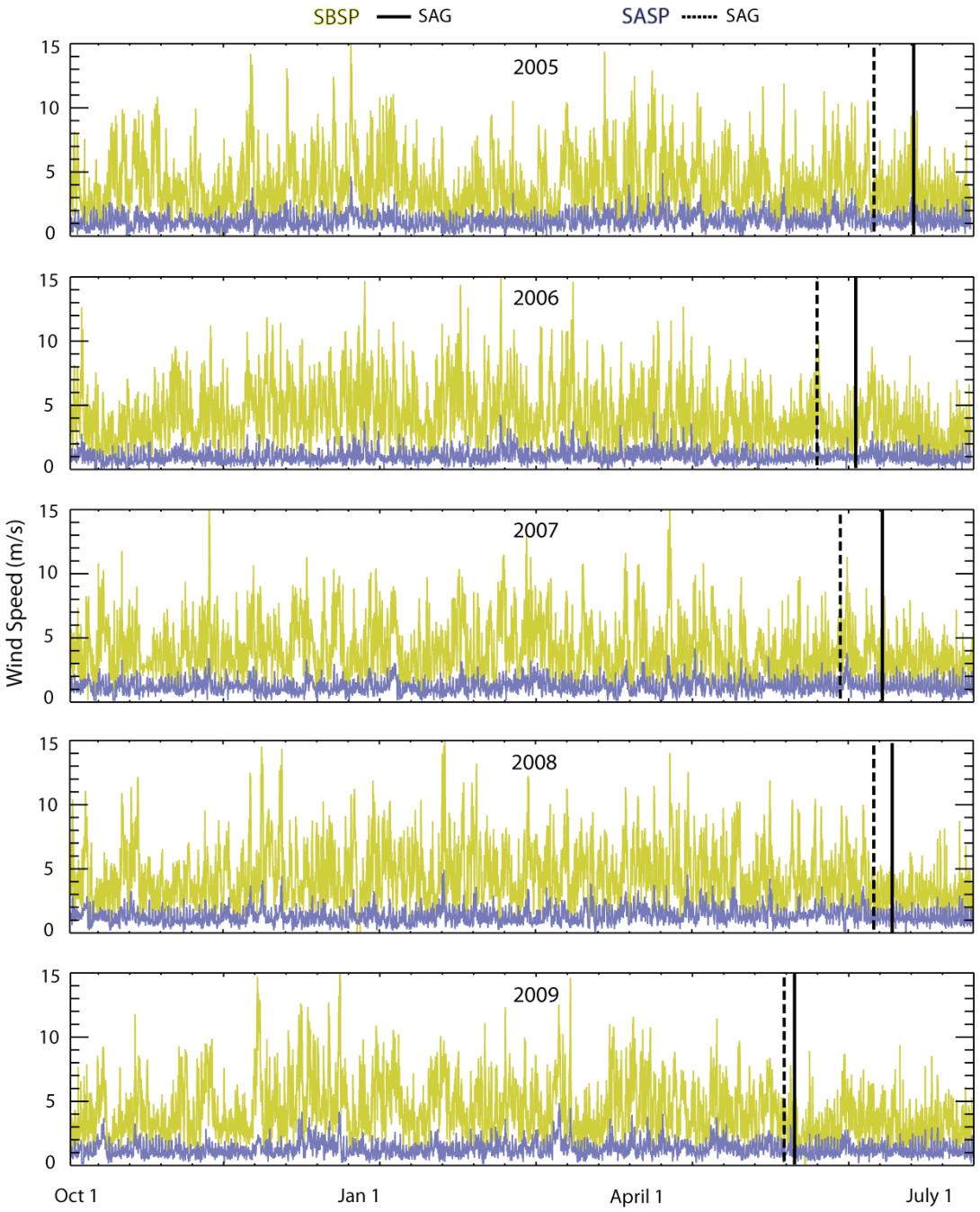

E.

Figure 4 continued.

Table 4 The range and accuracy of the instruments used to measure the energy balance parameters at the towers.

Measured Parameters	SBSP (alpine)	SASP (subalpine)
Air temperature *	•	•
Relative Humidity *	•	•
Wind Speed *	•	•
Precipitation		•
Incident/Reflected Broadband Shortwave Radiation	•	•
Incident/Reflected NIR/SWIR Radiation	•	•
Longwave Irradiance	•	•

* at two heights

CHAPTER 4

RESULTS AND DISCUSSION

The results of this study are described below. Results from observations and measurements are described first. The observed results address interannual variation in dust in snow radiative forcing (research question 1). Results from snowmelt modeling are then described, which address the relationship between melt out date and dust in snow radiative forcing in snow at a seasonal scale (research question 2), and the relative capacity of radiative forcing by dust and temperature to accelerate snowmelt (research question 3). Finally, sensitivity and uncertainty results are described.

Interannual Variability

Dust Concentrations

Figure 5 shows end of year dust concentrations at SBSP (A) and SASP (B), and the number of recorded dust events per year since 2003 is shown in Figure 6. These figures collectively illustrate that dust concentrations are not necessarily related to the number of dust events. This is because the amount of dust entrained and deposited by each event varies depending on conditions such as the intensity and duration of the wind event and the vulnerability of soils in the source regions. In Figure 6, the red bars indicate total number of dust events per year and the black bars indicate the number of events that

occur after March 1st, during the critical spring melt season. The number of dust deposition events has increased monotonically since 2005, whereas the greatest dust loadings occurred in 2006 and 2009, with 2009 being a factor of 5 greater then 2006 and up to 20 times greater than the other years. This is true even for 2009 in relation 2008 when the same number of dust events was recorded after March 1st but the dust concentration was an order of magnitude greater in 2009.

Radiative Forcing

Cumulative solar irradiance and cumulative radiative forcing was calculated from measurements collected at the towers over the ablation seasons of 2005 through 2009, which is defined as the difference between the date of average peak SWE and average melt out date. Cumulative radiative forcing and cumulative broadband solar irradiance are plotted for SBSP and SASP in Figure 7 and Figure 8, respectively. The short time period plotted is due to lack of sensor measurements at the end of the 2009 winter season at SBSP, but the time period includes measurements through the depletion of snow for 2009.

Despite the lower cumulative irradiance in 2009, which experienced a higher number of cloud-covered days over the ablation season than the other years (which resulted in a lower cumulative irradiance), the radiative forcing from dust was markedly greater than the other years. This demonstrates the magnitude of the dust impact; if the lower cumulative solar irradiance had occurred in the absence of the dust loading, the radiative forcing would have been reduced, and the snowcover duration would have been extended. Alternatively, if the high dust concentrations of 2009 were experienced in a year with higher cumulative solar irradiance, additional enhancement of melt would have

been observed. These results indicate that the presence of dust exhibits a strong control on melt.

Figure 9 and Figure 10 show visible (A) and broadband (B) albedo evolution over the ablation season (15 April to snow all gone date) for SBSP and SASP, respectively. The lowest end of year albedo measurements recorded occur in 2009, the year with the highest dust concentration, greatest radiative forcing, and earliest melt out date. The earlier melt out is attributed to the decline in albedo, which happens relatively quickly in 2009 in comparison with the other years due to the greater radiative forcing experienced in the presence of high dust concentrations.

At SASP in 2009 snow albedo was distinctly lower than the previous years, and the reduction happened more rapidly. There was a reduction in visible albedo from 0.72 to 0.33 over 13 days (day of year 109 to 121), which is a difference of an additional 40% absorption of solar radiation. A precipitation event brought the albedo back up to 0.91 at day of year 122, but it dropped again to 0.33 within 5 days (day 127) and maintained a value of about 0.3 until melt out 11 days later (day 138). The snow surface was absorbing up to 70% of incoming solar radiation over this time period. The lowest average albedo over the ablation season was also observed at SASP at 0.49, with the average absorption over 50%. At SBSP there was a similar end of year decline in albedo, which was reduced from 0.9 at day 122 to 0.34 in 16 days (day 138) and melt out occurred within 2 days (day 140). Most literature cites snow albedo as ranging from 0.4-0.9, and 2009 would indicate values can be lower in the presence of dust loading.

The next most rapid deterioration of albedo and lowest albedo measurements occur in 2006, the next largest dust concentration year. For SASP this resulted in an end

of season reduction of albedo from an ablation season peak of 0.89 at day 129 to about 0.4 in 15 days (days 144) and melt out occurred within 2 days. The same precipitation event which raised the albedo at SASP to 0.89 also occurred at SBSP, which saw a reduction a similar reduction in albedo to 0.4 over 26 days (day 155) and melt occurred within 2 days.

Snowmelt Modeling

As described by Painter et al. (2007) the difference between observed and simulated melt out dates for the observed scenario ('dust case') provides a measure of the accuracy of SNOBAL. For years 2005 through 2009 modeled snow depletion occurred within 1 day of observed depletion at both sites with the exception of SBSP in 2005, where it was 2 days, which resulted from inaccurate partitioning of precipitation phase during a rain on snow event at the end of the snow cover season.

Comparison of model results with measurements of SWE recorded at the study plots provides another measure of accuracy of SNOBAL. Measured SWE is closest to modeled SWE at SASP, with a RMSE of 74.6 mm. The difference between measured and modeled SWE was slightly higher at SBSP, with an RMSE of 137.6 mm. The variation for SBSP is attributed to known differences in terrain characteristics at the study plot; the snow depth is typically deeper at the location where the snow pits are dug than at the tower. The average difference between depth recorded by the snow depth sensor at the tower, and the depth recorded at the snow pits is about 20 cm difference over all pits and years. The magnitude of the variation is addressed by calculating observed SWE from sensor snowdepth and density recorded at the snowpit, these values are plotted over modeled SWE in Figure 11. The average difference in SWE calculated from snowdepth

recorded at the snowpits and depth recorded at the tower is 86.6 mm over all years. This could potentially cause issues with SNOBAL because the model is initiated with measurements from the snowpits, and forced with data measured at the tower. This is considered acceptable, though, because melt is still accurately simulated within a day of observed melt for all years except 2005, as discussed above.

Snow Water Equivalent (SWE)

Figure 11 and Figure 12 show the time series of snow water equivalent during the ablation season (15 April to 20 July) for 2005 through 2009 for SBSP and SASP, respectively. The red curves ("Dust now") represent the observed 'dust case' whereas the lightest blue curves ("Clean snow now") represent the SWE evolution for the 'clean case'. The darker blue curves represent the time series of clean SWE under the scenarios of increases in temperature. The yellow and orange curves represent the time series of dust case under the scenarios of increases in temperature.

The difference between where the red curve and the lightest blue curve intercept the x-axis represents the number of days that dust advances melt under current climate conditions; the greatest divergence between dusty snow and clean snow is 50 days at SASP and 41 days at SBSP. The largest divergence occurred in 2009 when end of year dust loading was 5-20x greater than that during the previous 4 years. The next largest divergence at SASP of 31 days occurred in 2006, the next largest dust concentration year. The years with lower dust concentrations; 2005, 2007, and 2008, still show advancement of melt of 26-30 days at SASP and 21-27 days at SBSP relative to clean case.

In 2005 the advancement of melt, relative to the clean case, was 28 days for SASP and 23 days for SBSP. In 2006 the modeled subalpine melted out completely 31 days

earlier and the alpine 21 days earlier. In the alpine this was lowest difference between the dust and dust free cases, even though it was still the second highest dust concentration year. As was discussed in Painter et al. (2007) the higher peak snow water equivalent in 2005 relative to 2006 resulted in the small difference between the two years, with respect to snow cover durations, despite the increase in dust concentration and radiative forcing. A larger difference in melt rates may have been observed if snow water equivalent had been higher and snow cover duration longer in 2006.

The difference between the light blue curve and darker blue curves represents the number of days temperature increases would advance melt in the absence of dust. The difference between the temperature change driven melt and the dust driven melt advance indicates the markedly greater capacity of present-day dust loading to influence snowmelt relative to an air temperature increase of either 2^{o} or 4°C.

The difference between the red curve and orange and yellow curves represents the number of days temperature increases would accelerate melt in the presence of dust. In comparison to the clean snow temperature increase curves these curves show that in the presence of dust temperature increases are less effective at forcing snowmelt than were they to occur in the absence of dust. This is because dust radiative forcing reduces SWE, and in turn reduces the period over which changes in temperatures can have an impact on snowmelt. The scenarios used to create these plots are summarized in Table 3. Results for temperature increases are discussed in more detail below.

Snow All Gone (SAG) Date

Change in the snow all gone (SAG) date is the difference between the modeled melt out dates for the dust and clean snow cases. The clean snowpack is modeled by

removing the minimum and maximum radiative forcing due to dust, with the mean of these two scenarios considered to represent a clean snowpack, representing our best understanding of the evolution of the snowpack in the absence of dust.

Change in SAG, the difference between the clean and dust case, represents the number of days that dust radiative forcing advances melt. Figure 13 plots change in SAG for both sites for 2005-2009. The red bars on these plots represents the number of additional days were this to be calculated from the clean case with maximum radiative forcing removed (versus the average of the maximum and minimum cases), considered the upper bound on the maximum impact of dust radiative forcing on melt out date. Figure 14 shows changes in SAG with dust concentration. These plots show that, on average, change in SAG increases with increasing dust concentration.

Runoff

Figure 15 and Figure 16 plot the evolution of daily runoff over the ablation season at SBSP and SASP, respectively. The colors used for these curves are as described for the SWE figures above.

Runoff reaches zero when the snow cover has been depleted. These results are similar to the SWE results except that as snow melts SWE is depleted; not all melt water becomes runoff. Water can infiltrate into the column soil, be transpired by vegetation, and evaporate. SNOBAL models melt and evaporation; the difference between these two is considered the runoff. This is runoff as modeled at a point, which may be more accurately described as snowpack outflow.

For all years at both sites for observed conditions, or dust case (red curve), melt out occurs more rapidly relative to the clean case (lightest blue curve) with earlier and

higher peak runoff. For both sites and all years temperature increases in the absence of dust advance runoff timing but these advances are small relative to the advancement of runoff due to dust. The way in which SNOBAL handles precipitation events after melt out for observed conditions may not accurately represent what would occur in the absence of dust, i.e., rain on snow events that cause a large increase in modeled runoff, this will require further investigation and is beyond the scope of this thesis. For both sites and all years temperature increases in the presence of dust advance melt by 1-4 days, except in 2009 where runoff occurs on the same day for all three scenarios. In the presence of heavy dust loading the runoff occurs rapidly such that temperature increases do not impact runoff timing.

Temperature Changes

Change in SAG for observed conditions ("Now") at both SASP and SBSP is represented by the black bars in Figure 17 with added days difference of modeled 2° and 4° C temperature increases in orange and yellow ("Plus 2","Plus 4"). These plots show that in the presence of dust temperature increases have a smaller impact on melt out date than in the clean maximum and minimum forcing cases. The smallest impact from modeled temperature increases in the dust case is in 2009 at SASP, corresponding to the largest dust concentration of any year. Effectively there is no impact from temperature increases in the presence of such heavy dust loading.

Figure 18 shows change in SAG ("Now") relative to change in SAG for modeled clean 2° and 4° C temperature increases ("Clean Plus 2","Clean Plus 4") at SASP and SBSP. These plots show that warming by 2° and 4° C has a larger impact on change in

SAG in the absence of dust but has less melt capacity. The scenarios used to create these plots are summarized in Table 3, and a summary of the results is shown in Table 5.

Sensitivity and Uncertainty

Figure 19 shows time series of SWE over the ablation season for the ranges in instrument accuracies using the observed dust case for the 2007 ablation season at SASP. The greatest sensitivity of 2 days difference in SAG by the end of season occurred with the longwave irradiance, which has an uncertainty of ±3%. The next largest change occurred for net solar radiation and wind with almost a 1-day difference for each parameter. The sensitivity for air temperature, vapor pressure, and precipitation were near zero with the exception of an increase in precipitation that resulted in ¼ day later melt. The days difference for each range in accuracy is summarized in Table 6, where negative numbers represent earlier melt and positive numbers represent later melt. Figure 20 is modeled SWE evolution for all parameters and their respective ranges in accuracy, representing the maximum uncertainty involved with instrument measurements, which is 2 days for max accuracy range (+) and 3 days for minimum accuracy range (-).

Changes in SAG due to changes in surface roughness are plotted in Table 7 and Table 8 for SBSP and SASP, respectively. The number of days difference shown in the table represents advanced melt. Due to the low wind speeds recorded at SASP the model would not run for 5 cm enhanced surface roughness. For increased surface roughness of 5 mm in the dust case at both sites melt is either not impacted, or advanced by 1 day. The largest difference in melt out occurs for the clean case at both sites, for a modeled clean snowpack increases in surface roughness can enhance melt by 3 to 7 days at the alpine

site and 1 to 4 days at the subalpine site. These results indicate that the impacts from increased turbulent transfer at the surface in the presence of dust are reduced due to shorter snow duration.

At SBSP, there is a threshold between 1 cm and 5 cm increased surface roughness where large difference in melt out date occurs. The larger advances in melt for 1 cm and 5 cm increased roughness occur for both the dust and clean cases at SBSP can be attributed to the higher wind speeds, which increases turbulent transfer, occurring at the alpine site. The use of 1mm constant surface roughness is considered acceptable as these results indicate the model is not highly sensitive to changes in surface roughness until roughness values increase beyond commonly observed surface roughness values.

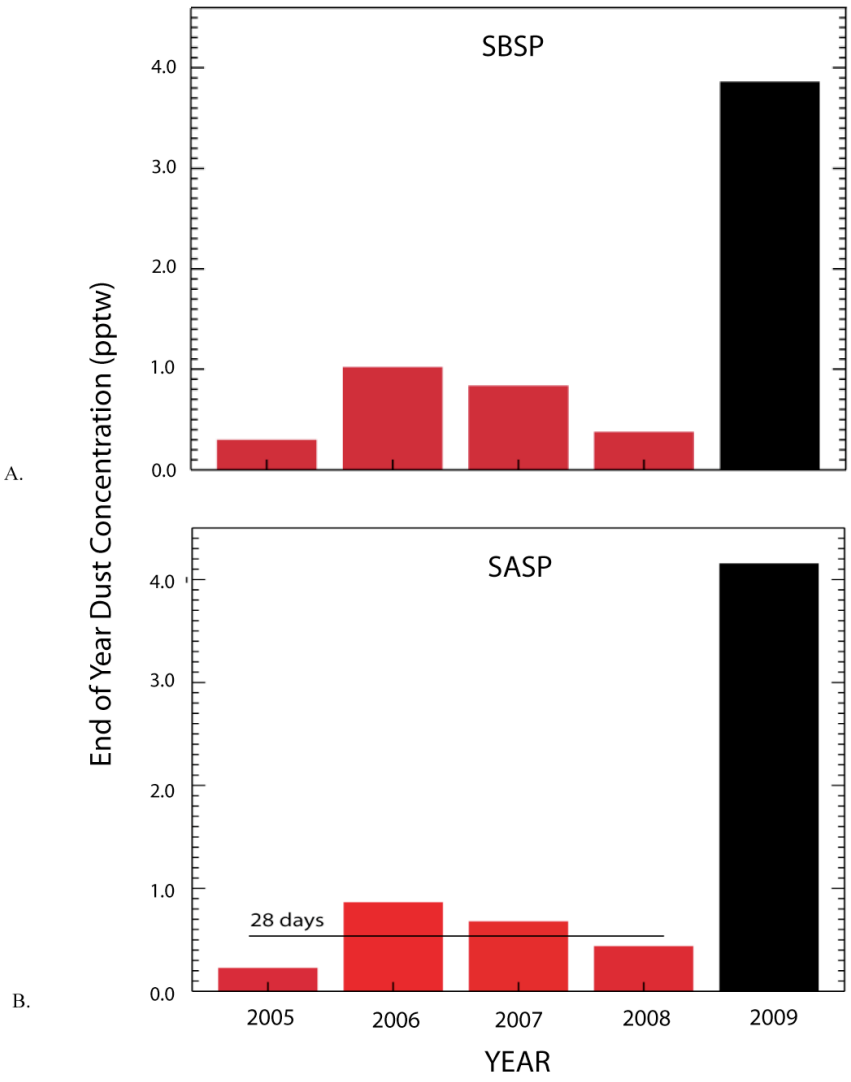

Figure 5 End of year dust concentrations at SBSP (A) and SASP (B). Average number of days of advanced melt is given for SASP for 2005 -2009, for reference. In comparison, the advanced melt for 2009 was 41 days (SBSP) and 50 days (SASP). 2009 is represented by a black bar to highlight the large dust concentration relative to the other years.

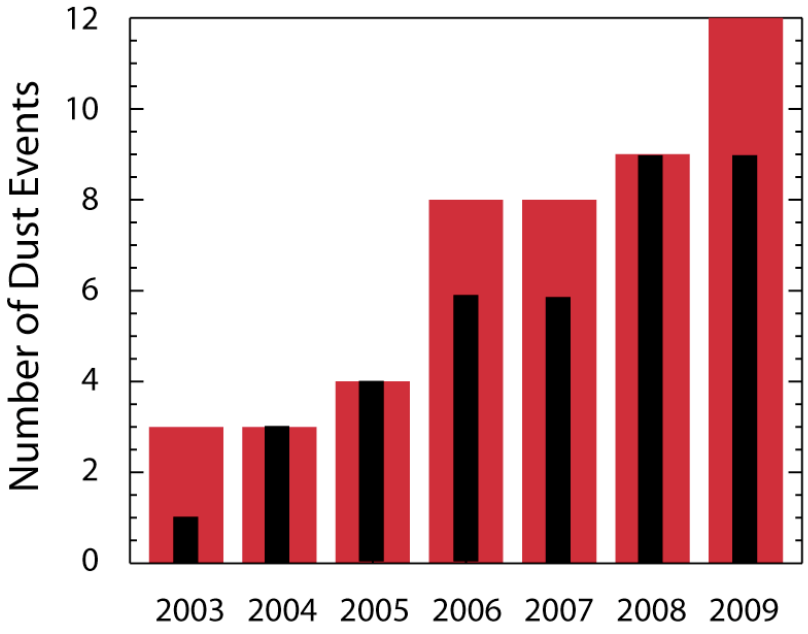

Figure 6 Number of observed dust events per year for Senator Beck Basin Study Area since observations began in 2003, red bars are events per year and black bars are events after March 1st.

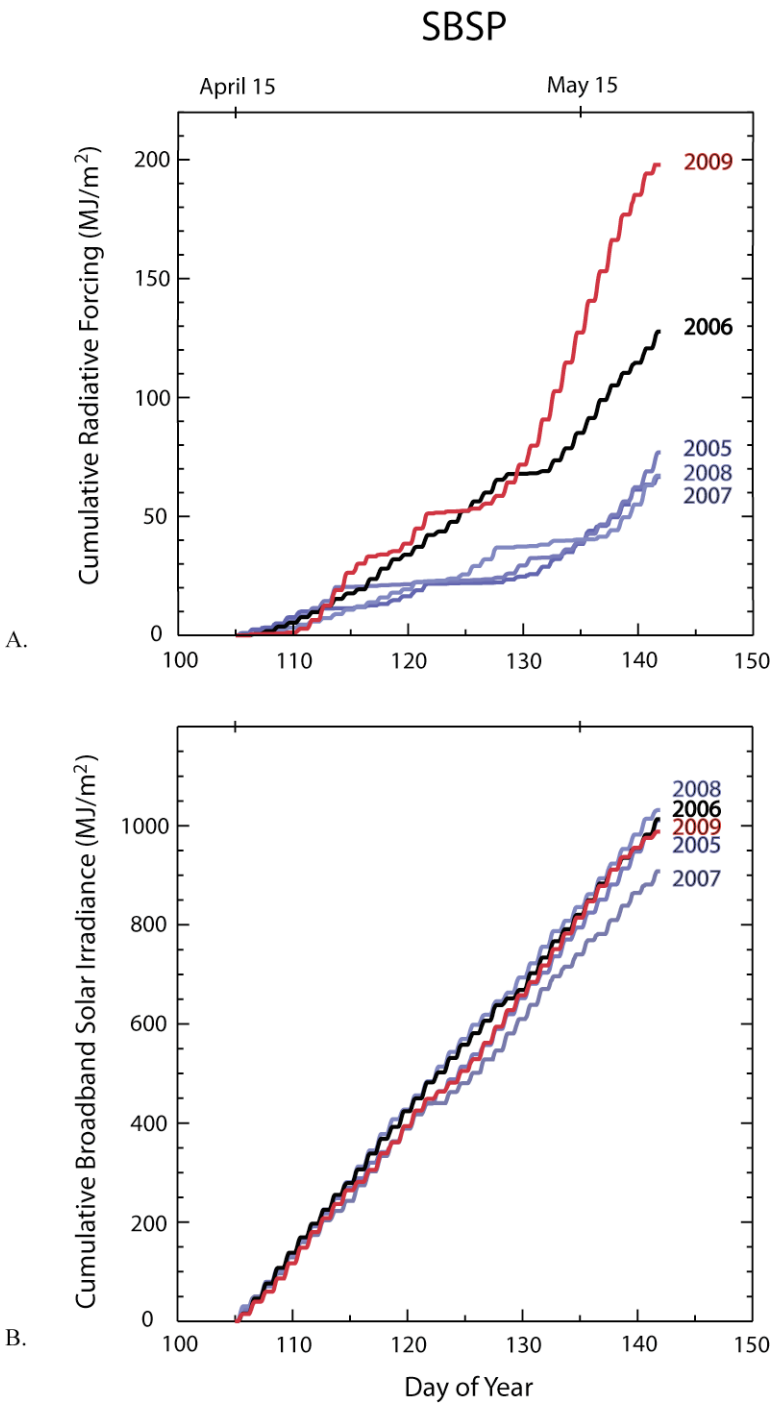

Figure 7 Cumulative radiative forcing (A) and broadband solar irradiance (B) measured at the SBSP tower.

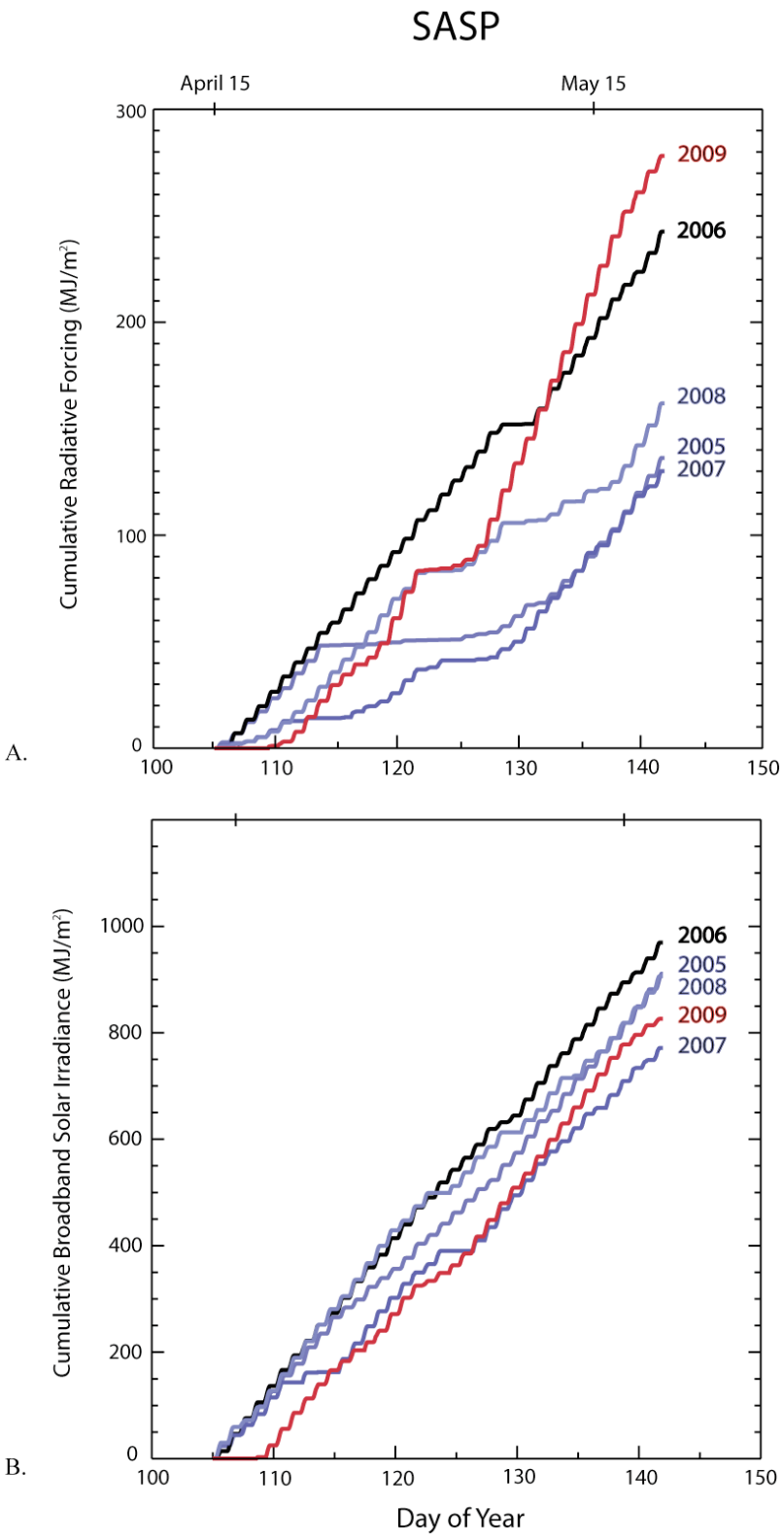

Figure 8 Cumulative radiative forcing (A) and broadband solar irradiance (B) over the ablation season at the SASP tower.

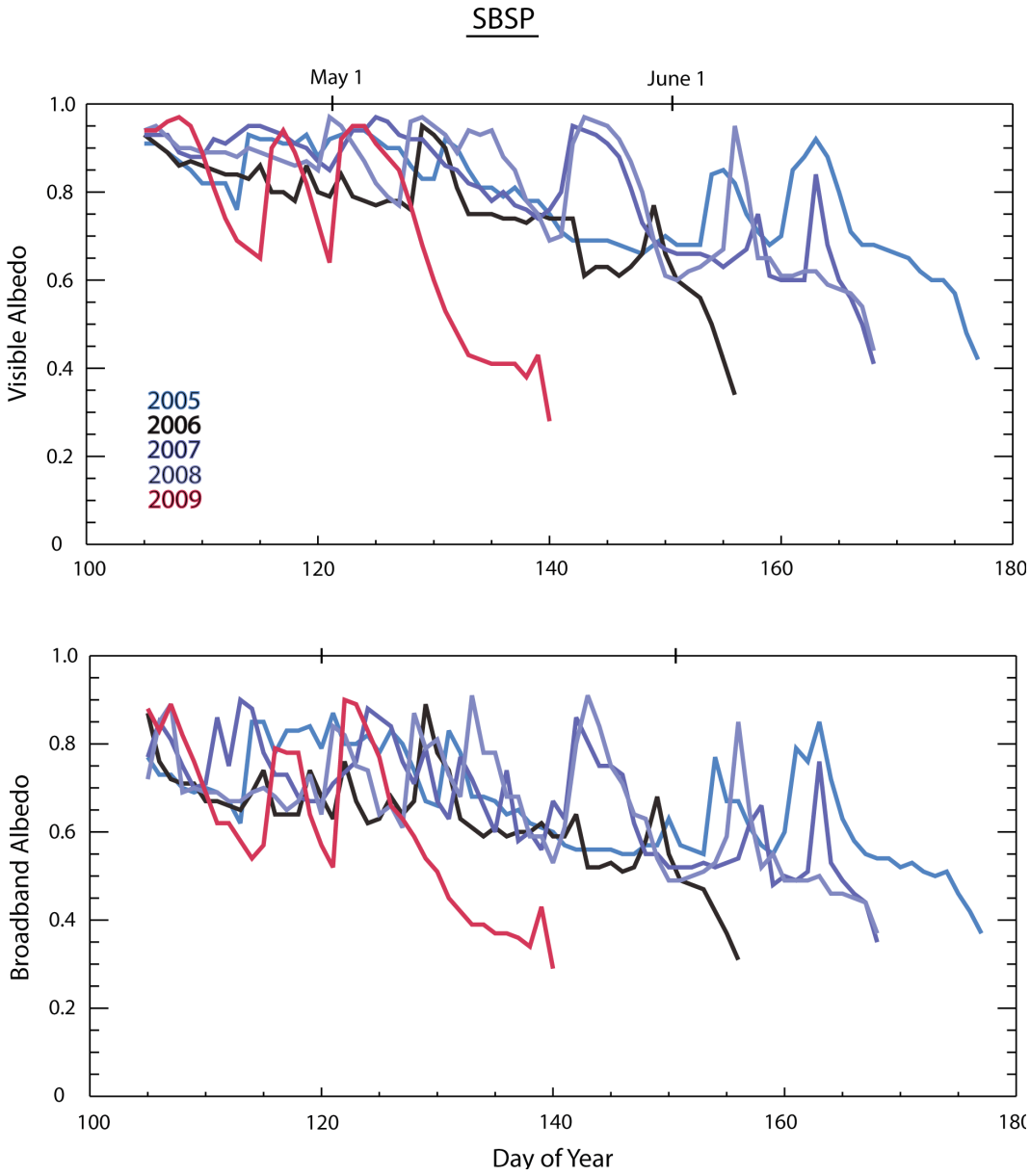

Figure 9 Evolution of visible (A) and broadband (B) albedo over the ablation season at the SBSP tower.

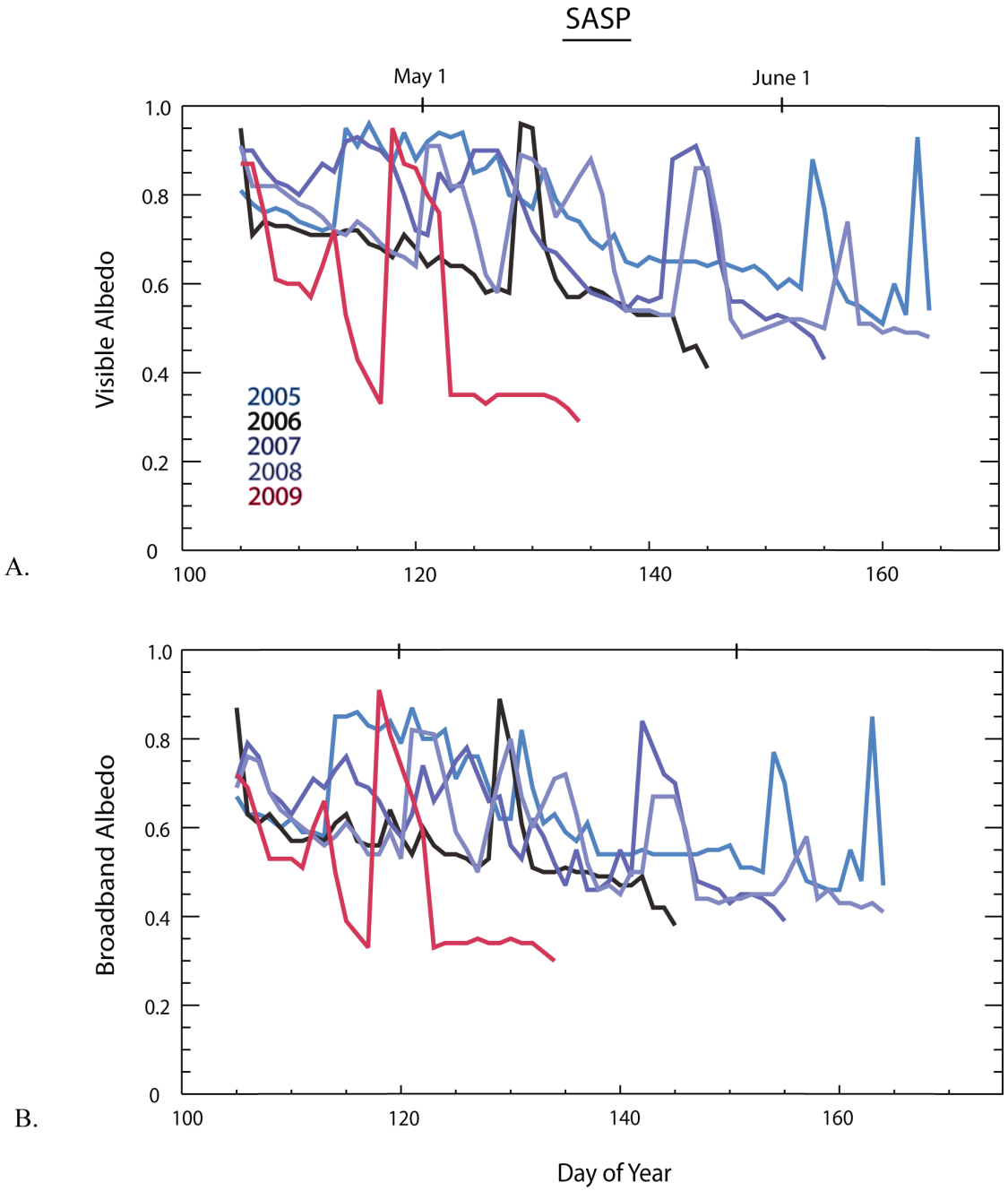

Figure 10 Evolution of visible (A) and broadband (B) albedo over the ablation season at the SASP tower.

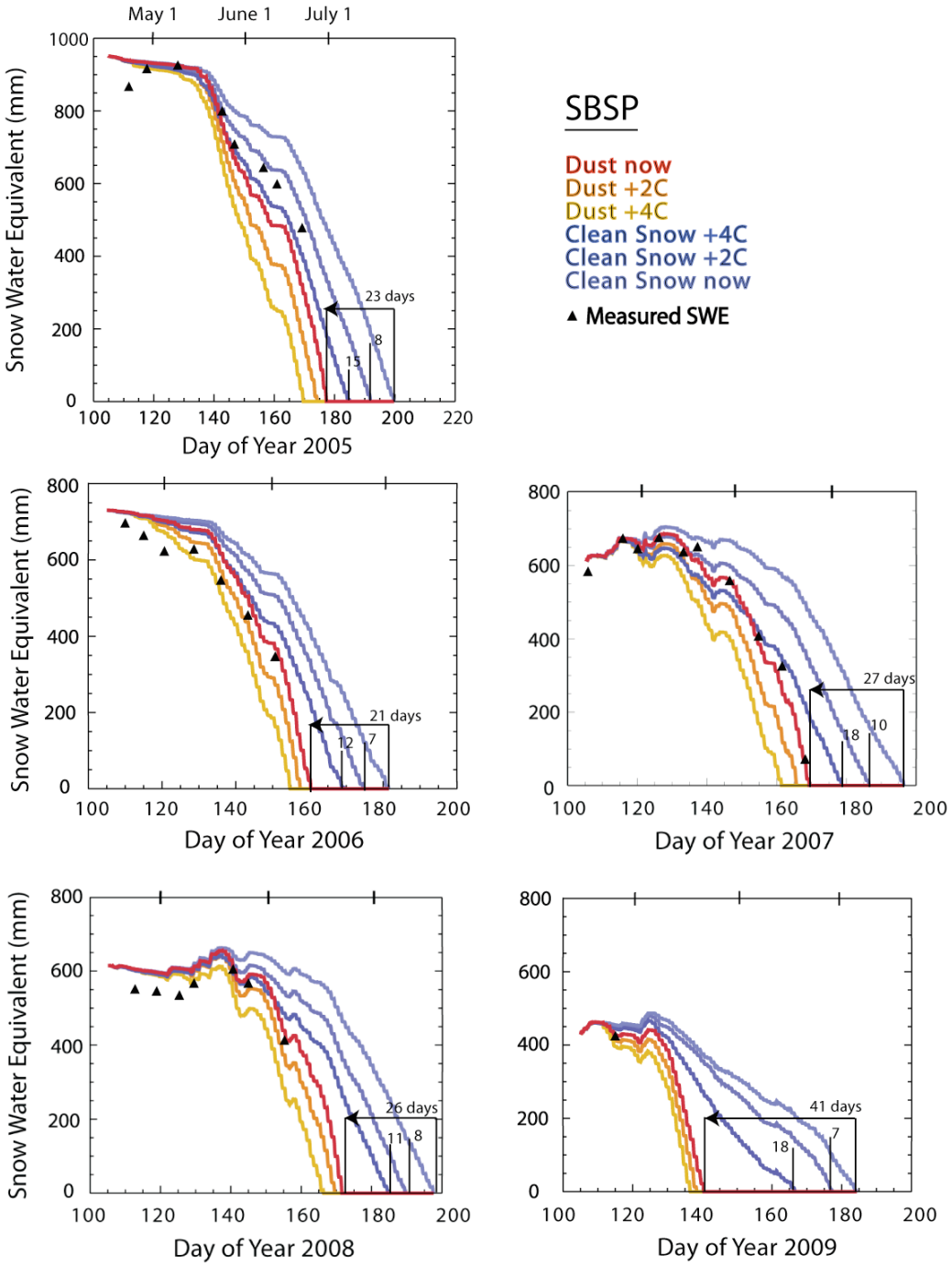

Figure 11 Modeled SWE evolution over the ablation season at SBSP. Measured SWE calculated from snow depth sensor and snow density recorded at the snow pits, how closely these match the modeled SWE evolution (red curve) gives an indication of the accuracy of SNOBAL.

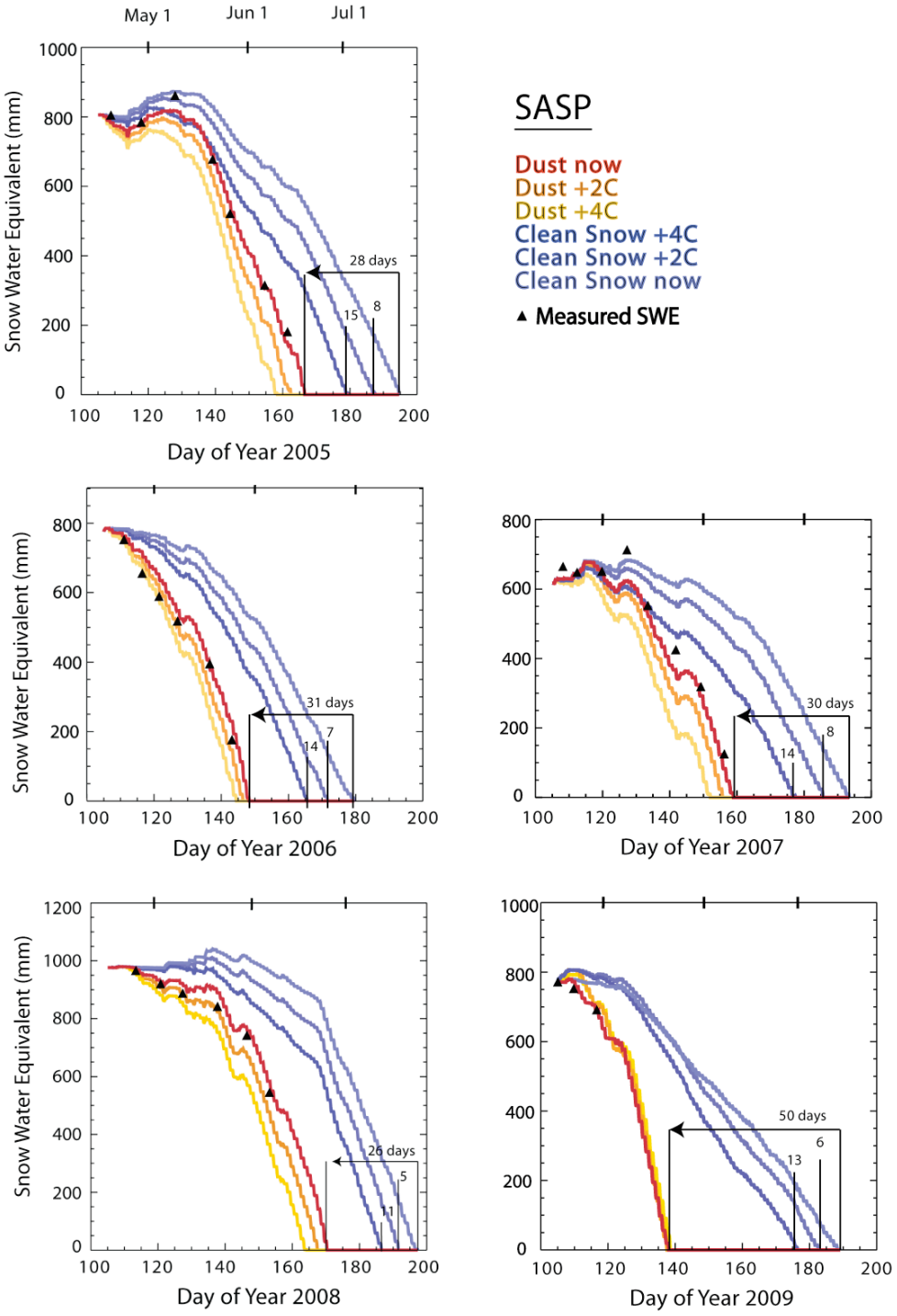

Figure 12 Modeled SWE evolution over the ablation season for all scenarios. In almost all cases modeled SWE evolution for observed conditions (red curve) closely matches the point measurements of SWE recorded at the study plot, indicating that SNOBAL accurately simulates actual conditions.

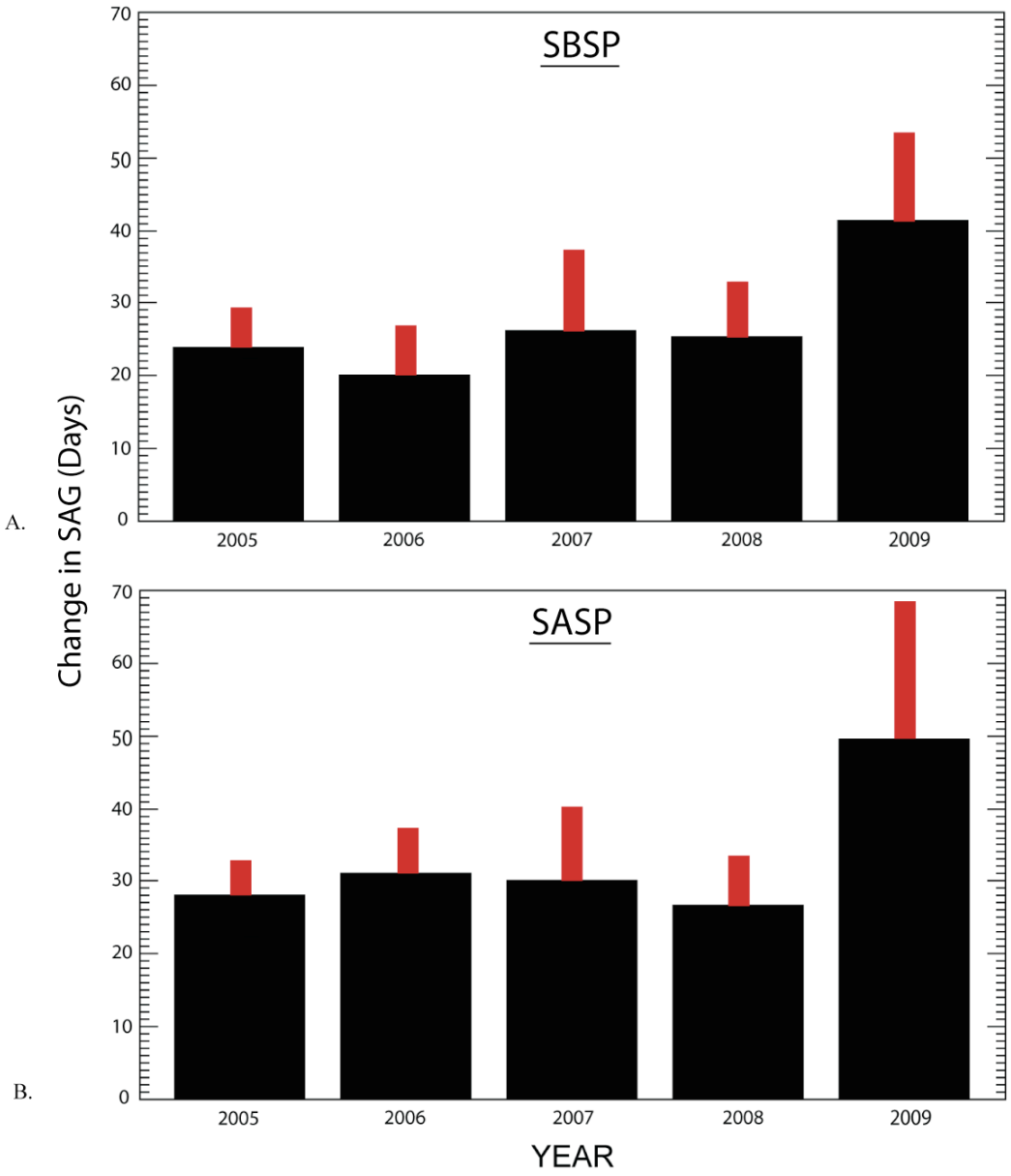

Figure 13 Change in snow all gone date (SAG) at SBSP (A) and SASP (B). Black bars are the difference between clean and dust case; red bars are the difference between max forcing clean case and dust case, representing the largest potential change in SAG.

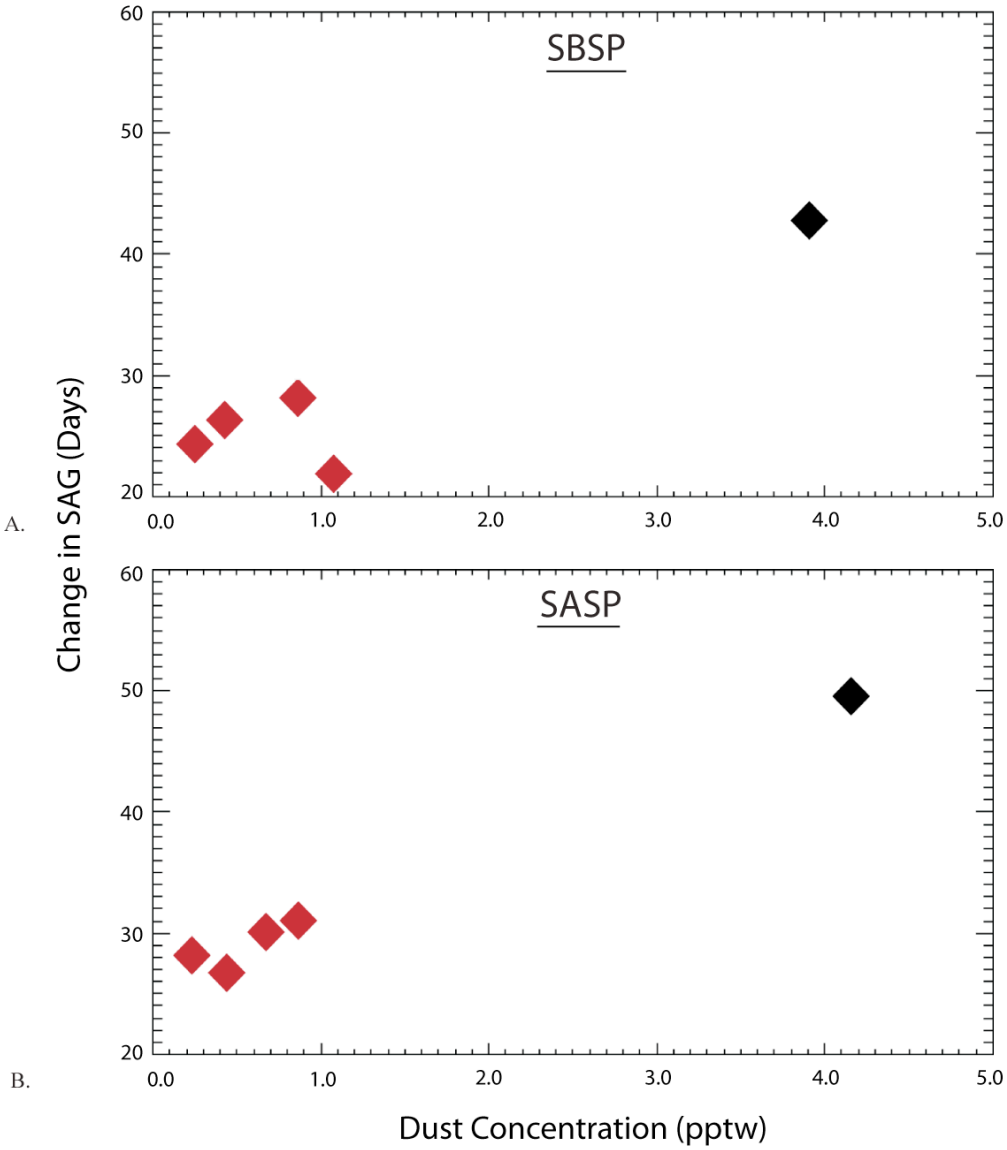

Figure 14 Change in snow all gone date (SAG) with end of year dust concentration at SBSP (A) and SASP (B), in general change in SAG increases with increasing dust concentrations (linear relationship), the exceptions being 2006 at SBSP and 2008 at SASP. Black diamonds are 2009, the year with the highest dust concentration and largest change in SAG.

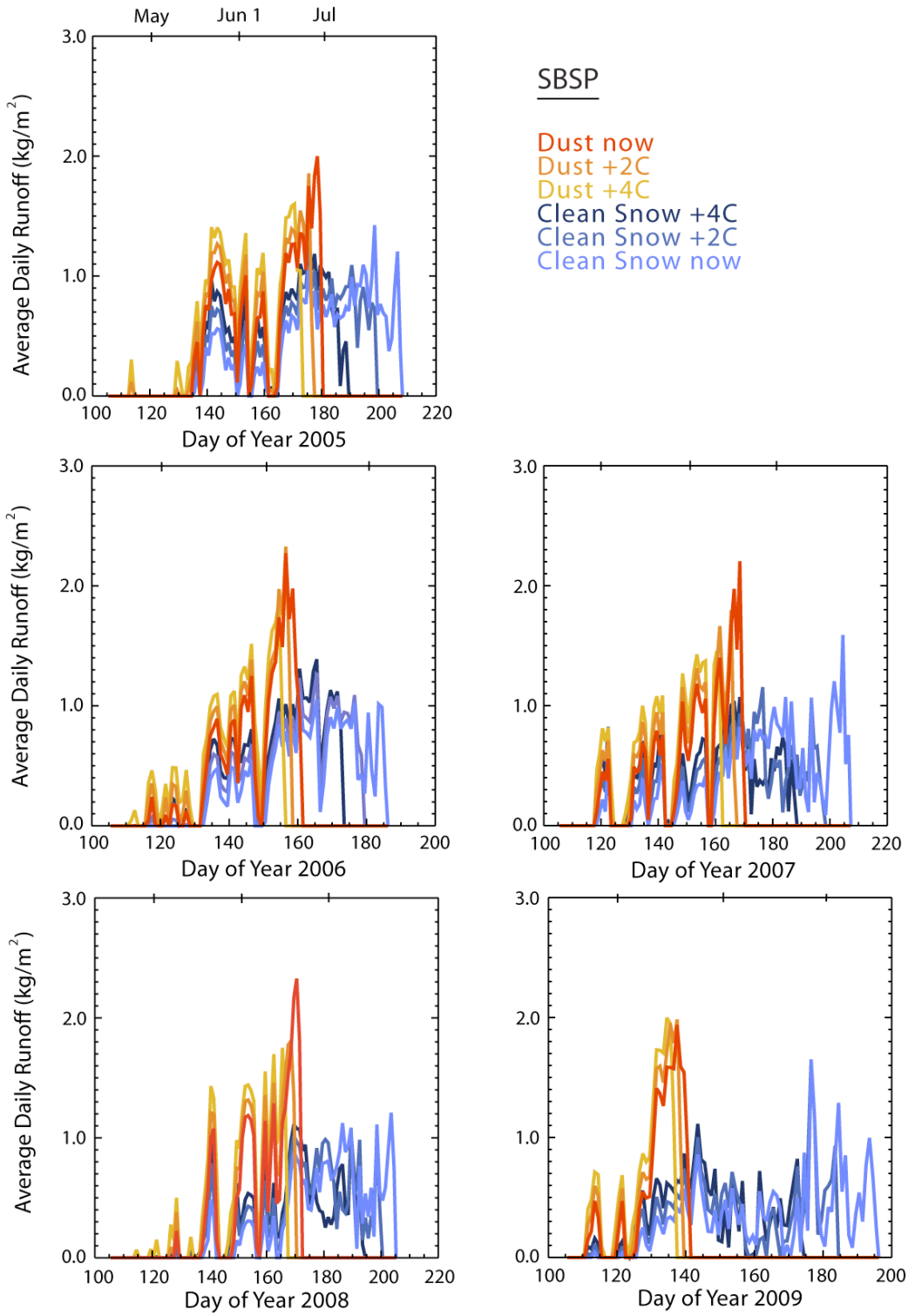

Figure 15 Modeled runoff under all scenarios at SBSP. For all years the dust and dust plus temperature increase scenarios result in earlier and higher peak runoff, the largest difference between dust cases and clean cases occurs in 2009, the year with the highest end of year dust concentration.

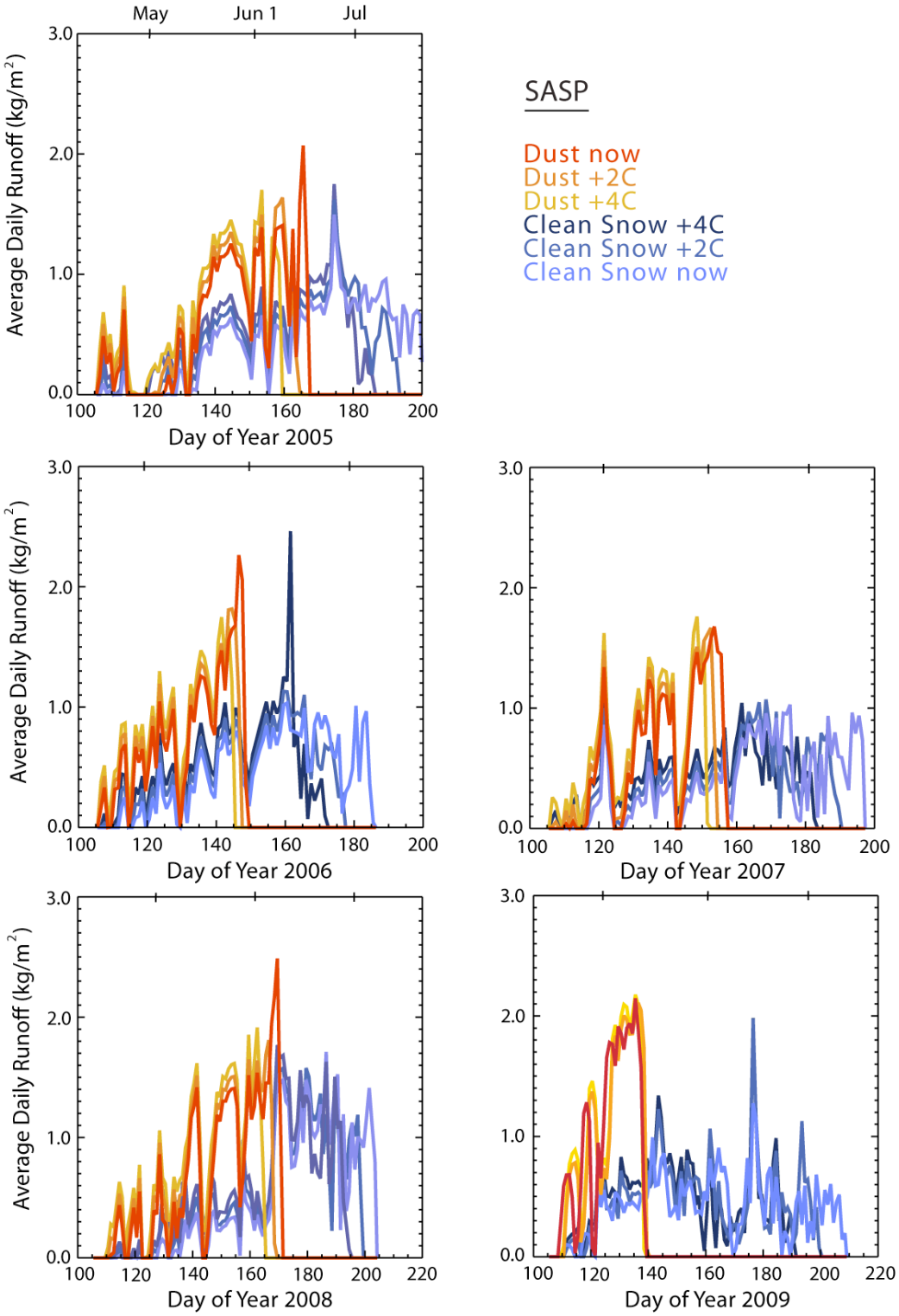

Figure 16 Modeled runoff for all scenarios at SASP. For all years the dust and dust plus temperature scenarios result in earlier and higher peak runoff, as at SBSP the largest difference between dust cases and clean cases occurs in 2009.

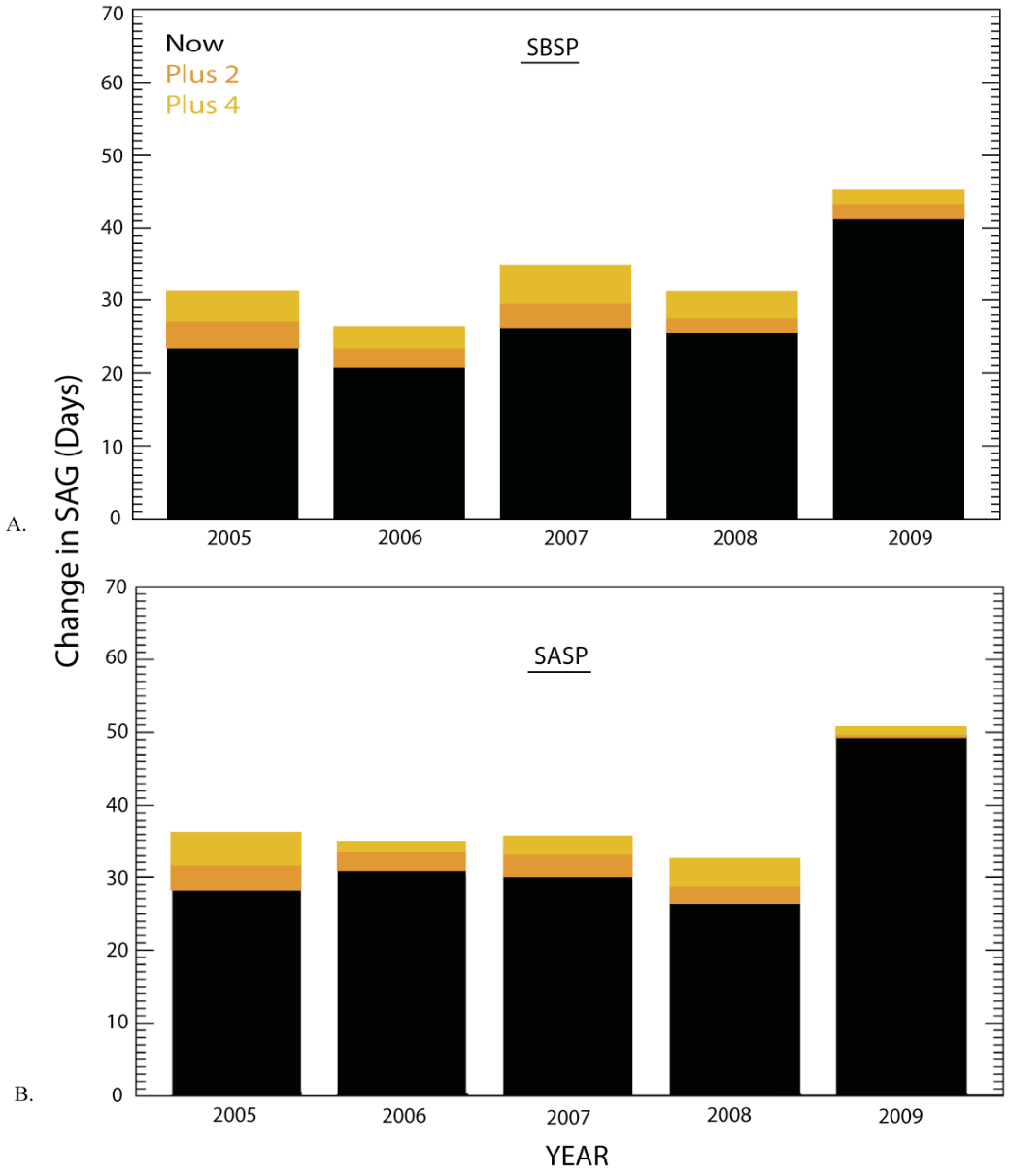

Figure 17 Change in SAG (black bars) with additional days change in SAG due to temperature increases of +2^{o}C (orange bars) and +4^{o}C (yellow bars) at SBSP (A) and SASP (B).

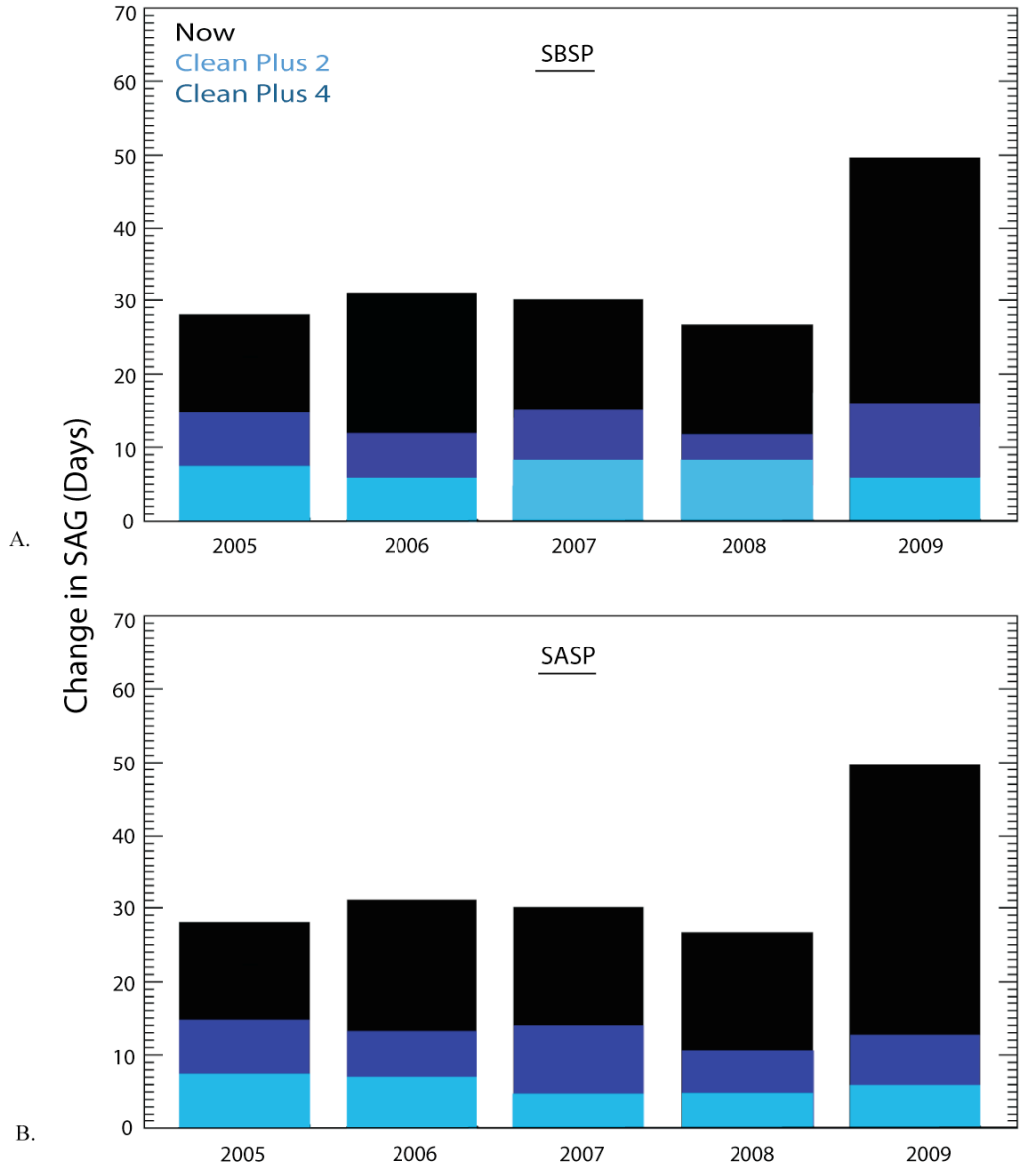

Figure 18 Change in SAG for observed conditions (black bars) in comparison to change in SAG for the clean case with added temperature increases of +2^{o}C (light blue bars) and +4^{o}C (dark blue bars) at SBSP (A) and SASP (B).

Table 5 Summary of number of days advanced melt for various scenarios in comparison to the clean case.

Number of Days of Advanced Melt (Temperature Increases)					
	Dust	Dust +2°C	Dust +4°C	Clean +2°C	Clean +4°C
SASP	26 - 50	0 - 2	1 - 7	5 - 8	11 - 15
SBSP	23 - 41	2 -3	3 - 8	6 - 8	12 - 18

Table 6 Summary of days difference in melt due to varying the measured parameters to their respective accuracy ranges.

Instrument Accuracy (Days Difference)		
	Plus	Minus
Net Solar Radiation	-0.88	0.83
Longwave Irradiance	-1.92	2.12
Air Temperature	-0.04	0.04
Vapor Pressure	-0.04	0.04
Wind Speed	-0.83	0.83
Precipitation	0.25	-0.04

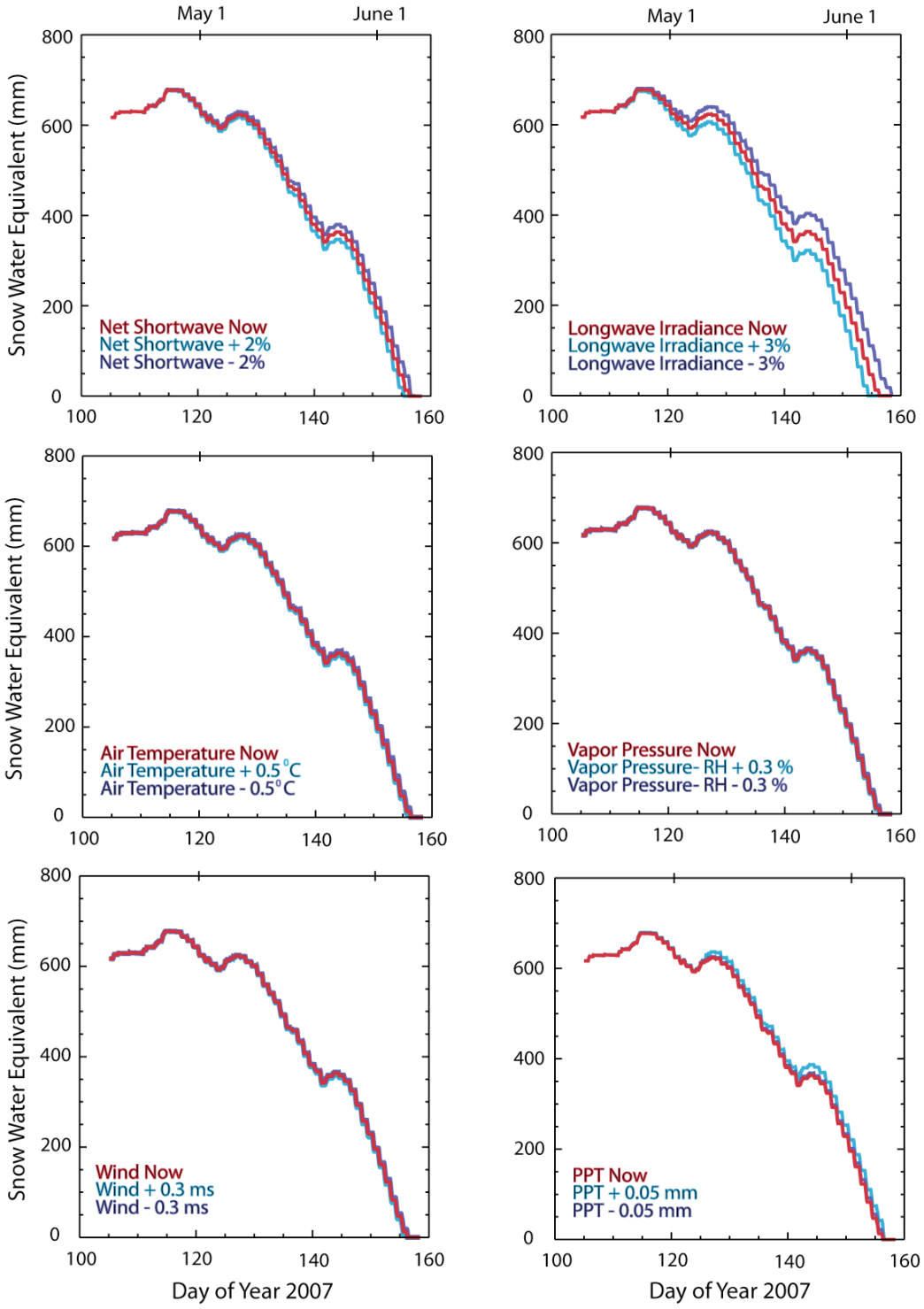

Figure 19 Modeled SWE for range in instrument accuracy, over the 2007 ablation season at SASP. The red curve is SWE evolution for observed conditions; the light and dark blue curves are modeled SWE the upper and lower accuracy range values, respectively. These plots represent the ranges for uncertainty due to instrument accuracy that is associated with each parameter.

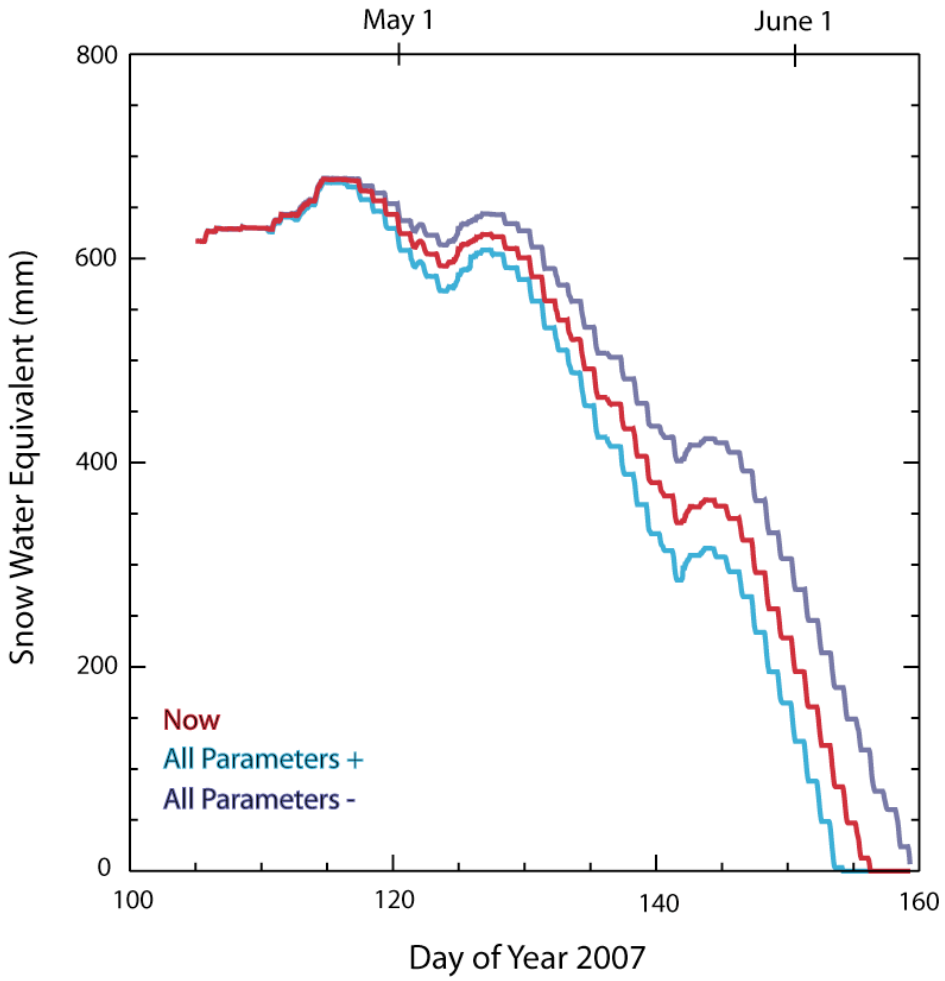

Figure 20 Modeled SWE evolution over the ablation season, for 2007 at SASP, with all forcing variables altered for accuracy range. This plot represents the maximum uncertainty attributed to instrument accuracy.

Table 7 Summary of advanced melt due to increasing surface roughness values for observed condition model runs at SBSP (A) and SASP (B). Wind speeds at SASP are too low for the model to run with a surface roughness of 5cm

A.

Surface Roughness Sensitivity (Days Difference)						
SBSP	Dust 5mm	Dust 1cm	Dust 5 cm	Clean 5mm	Clean 1cm	Clean 5cm
2005	1	1.5	19	4	7	28
2006	0	1	5.75	3	5.5	17.5
2007	1	2.75	—	7	11	—
2008	1	1	16	6	9	30
2009	0	0	2	4.5	6.5	—

B.

Surface Roughness Sensitivity (Days Difference)						
SASP	Dust 5mm	Dust 1cm	Dust 5 cm	Clean 5mm	Clean 1cm	Clean 5cm
2005	0	0	—	1	1.5	—
2006	0	0	—	1	1	—
2007	1	1	—	2	3	—
2008	0	0	—	2.5	4	—
2009	0	0	—	3	4	—

CHAPTER 5

CONCLUSIONS

Results have indicated that end of year dust concentrations are not necessarily related to the number of dust events. While modern dust levels are a relatively new phenomenon in this region over the last 150 years, we have observed a monotonic increase in the number of dust events over the 5-year record at our study area with variability between the amount of dust that is deposited from year to year. Our modeling results indicate that the number of days that dust advances melt and cumulative radiative forcing are linearly related to total dust concentration. For all years dust advances melt relative to a clean snowpack, by about a month for most years. This impact can be as great as almost 2 months as was modeled for 2009, the year with the highest end of year dust concentration.

Dust radiative forcing in the CRB has a markedly greater impact on snow cover duration than increases in temperature. While impacts from temperature and dust are mostly independent of each other, they occur at the same time. Temperature has little impact on advancing melt in the presence of heavy dust loading. The depletion of the snowpack is enhanced by the presence of dust such that temperature increases do not have the time to impact melt as strongly than in the absence of dust. In the scenario where dust deposition is curtailed our results indicate that temperature increases of 2^{o}C - 4^{o}C could enhance melt by 2-15 days relative to clean snowpack with observed longwave

radiation and air temperatures. While these results are based on simplifying assumptions they act as a starting point in quantifying the potential effects of climate change in the presence of dust loading in alpine snow cover, which has not yet been done.

Significance of Findings

Climate and atmospheric circulation vary at multiple spatial and temporal scales. In addition to natural variability, human impacts such as changes in land use and increased GHG emissions are contributing to changes. Climate and land use changes influence dust generation and deposition patterns through changing precipitation patterns, drought, disturbance, and desertification. It is important to understand the interannual variability of dust deposition into mountain snow cover to gain a better understanding of the potential long-term impacts. Over the previous 5 years we have seen a monotonic increase in the number of dust deposition events, yet dust concentrations have varied by orders of magnitude during those years. For the 5 years of record we have shown that melt can be advanced by up to 50 days during a high dust concentration year, and even in lowest dust concentration years melt can be advanced by up to 26 days.

These results have important implications for runoff timing and magnitude, water supply, power generation, alpine phenology, forest fire regimes, and recreation. Painter et al. (2007) found that dust in snow can enhance snowmelt by up to 30 days, and this study found that in a high dust concentration year melt can be enhanced up to 50 days. This advanced melt impacts the timing and magnitude of peak runoff and subsequently impacts soil moisture storage and the amount of water lost to evapotranspiration, which can reduce available water supply (Painter et al., 2010). Painter et al. (2010) found that dust radiative forcing impacted annual runoff volume of the Colorado River between

1915 and 2003 at Lee's Ferry by 4.9% on average, corresponding to a cumulative loss in runoff of 85.71 bcm. Prior to the disturbance of the western US snow albedos would have been higher and snow cover would have lasted longer, and this water loss would not have occurred. If snow albedo can be as low as what was found in 2009 the impact of dust in snow on runoff may be even greater than the results indicate in Painter et al. (2010). Notably, the results of Painter et al. (2010) were based on an albedo parameterization that matches the albedos between 2005 and 2008, but not 2009, which had lower albedo and far greater absorption.

It is likely that the high dust concentrations observed in 2009 were due to reduced vegetation cover in the dust source regions that allowed for above average soil exposure. While the 2009 water year had average precipitation the months of August and September (2008) were very dry which led to low germination of winter annuals. January though March was also dry, which led to low growth rates. This combined to create low coverage and high exposure of vulnerable soils. As temperatures continue to increase and precipitation patterns shift the occurrence of drought in the southwest US is more likely and dust concentrations like those measured in 2009 may occur more often in the future.

Changes in runoff timing and subsequent changes in water supply are important impacts of reduced snow cover duration, especially in the Colorado River Basin where water supplies are over-allocated and where up to 70% of water supplies come from snowmelt (Christensen and Lettenmaier, 2007). There are additional impacts on the alpine environment such as changes in phenology and forest fire regimes. Steltzer et al. (2009) showed that the effects of earlier snowmelt due to dust synchronized the timing of greening and flowering across the landscape by melting snow cover and exposing the

vegetation prior to consistent temperature increases above 0^{o}C. Westerling at al. (2006) showed that reduced snowpack is associated with increased frequency and duration of wildfires. Reduced snow duration also directly impacts winter recreation by shortening the season and reducing snow quality. Changes in runoff can impact river recreation by altering peak runoff timing and timing of flow throughout the recreation season.

Future Work

The first step in increasing our understanding of the impacts from dust in snow is increasing the spatial extent of measurements in the western US with an expanded network of energy balance towers. Maintenance of current sites is also important: currently the temporal record is short, and additional years of measurements and observation will increase understanding of interannual variability of dust deposition into snow cover.

There have been considerable advances in monitoring climate and snow melt from ground stations, remote sensing, and point and distributed models (e.g. Marks and Winstral, 2001). Advances are being made in including dust radiative forcing into these methods. This study utilized a point snow energy balance snowmelt model, and having detailed radiation measurements at the two sites has increased our understanding of the impacts of dust in snow and allowed for comparison of impacts in alpine and subalpine environments. Terrain effects can significantly impact snow deposition, development of snow cover, and timing of melt much of which may not be captured in a point model. The next step is a spatially distributed melt model that incorporates dust radiative forcing at the basin scale to account for melt as a function of topography, wind, vegetation cover, and dust deposition.

Desert dust deposition into mountain snow cover is not only occurring in the western US. As discussed in the literature review dust deposition into snow cover is global in scale, and it is likely that earlier snowmelt and impacts on water resources are also occurring in these environments. The study of the impact of dust in snow should be expanded to include other regions around the world, in both seasonal snow cover and glaciated alpine environments.

REFERENCES

Asner, G.P. (2005). Grazing systems, ecosystem responses, and global change. *Annual Review of Environmental Resources, 29*, 38

Bales, R.C., Molotch, N.P., Painter, T.H., Dettinger, M.D., Rice, R., & Dozier, J. (2006). Mountain Hydrology of the Western United States. *Water Resources Research,42.*

Barnett, T.P., Adam, J.C., & Lettenmaier, D.P. (2005). Potential impacts of a warming climate on water availability in snow-dominated regions. *Nature, 438*, doi:10.1038/nature04141

Barnett, T.P., & Pierce, D.W. (2009). Sustainable water deliveries from the Colorado River in a changing climate. *Proceedings of the National Academy of Sciences, 106*, 7334-7338

Barnett, T.P., Pierce, D.W., Hidalgo, H.G., Bonfils, C., Santer, B.D., Das, T., Bala, G., Wood, A.W., Nozawa, T., Mirin, A.A., Cayan, D.R., & Dettinger, M.D. (2008). Human-induced changes in the hydrology of the western United States. *Science, 319*, 1080-1083

Belnap, J., & Gillette, D.A. (1998). Vulnerability of desert biological soil crusts to wind erosion: The influences of crust development, soil texture, and disturbance. *Journal of Arid Environments, 39*, 133-142

Betts, A.K., & Ball, J.H. (1997). Albedo over the boreal forests. *Journal of Geophysical Research, 102*, 8

Bohren, C.F., & Huffman, D.R. (1998). *Absorption and Scattering of Light by Small Particles*. New York: John Wiley and Sons, Inc.

Brock, B.W., Willis, I.C., & Sharp, M.J. (2006). Measurement and parameratization of aerodynamic roughness length variations at Haut Glacier d'Arolla, Switzerland. *Journal of Glaciology, 52*, 17

Christensen, N.S., & Lettenmaier, D.P. (2007). A multimodel ensemble approach to assessment of climate change impacts on the hydrology and water resources of the Colorado River Basin. *Hydrology and Earth System Sciences, 11*, 1417-1434

Christensen, N.S., Wood, A.W., Lettenmaier, D.P., & Palmer, R.N. (2004). Effects of climate change on the hydrology and water resources of the Colorado River Basin. *Journal of Hydroclimatology, 62*, 337-363

Conway, H., Gades, A., & Raymond, C.F. (1996). Albedo of dirty snow during conditions of melt. *Water Resources Research, 32*, 1713-1718

Cook, E.R., Woodhouse, C.A., Eakin, C.M., Meko, D.M., & Stahle, D.W. (2004). Long-term aridity changes in the western United States. *Science, 306*, 10.1126/science.1102586

De Angelis, M., & Gaudichet, A. (1991). Saharan dust deposition over Mont Blanc (French Alps) during the last 30 years. *Tellus, 43B*, 61-75

Dettinger, M.D., Cayan, D.R., Meyer, M.K., & Jeton, A.E. (2004). Simulated hydrologic responses to climate variations and change in the Merced, Carson, and American River basins, Sierra Nevada, California, 1900-2099. *Climatic Change, 62*, 283-317

Fassnacht, S.R., Williams, M.W., & Carrao, M.V. (2009). Changes in the surface roughness of snow from millimetre to metre scales. *Ecological Complexity, 6*, 9

Flanner, M.G., Zender, C.S., Hess, P.G., Mahowald, N.M., Painter, T.H., Ramanathan, V., & Rasch, P.J. (2009). Springtime warming and reduced snow cover from carbonaceous particles. *Atmospheric Chemistry and Physics, 9*, 2481-2497

Flanner, M.G., Zender, C.S., Randerson, J.T., & Rasch, P.J. (2007). Present-day climate forcing and response from black carbon in snow. *Journal of Geophysical Research, 112*

Franzén, L.G., Mattsson, J.O., Mårtensson, U., Nihlén, T., & Rapp, A. (1994). Yellow snow over the Alps and Subarctic from dust storm in Africa, March 1991. *Ambio, 23*, 233-235

Groisman, P., Karl, T.R., & Knight, R.W. (1994). Observed impact of snow cover on the heat balance and rise of continental spring temperatures. *Science, 263*, 2

Groisman, P., Knight, R.W., Karl, T.R., Easterling, D.R., Sun, B., & Lawrimore, J.H. (2004). Contemporary Changes of the hydrolgical cycle over the contiguous United States: trends derived from in situ observations. *Journal of Hhydrometeorology, 5*, 20

Hamlet, A.F., & Lettenmaier, D.P. (2005). Production of temporally consistent gridded precipitation and temperature fields for the continental United States. *Journal of Hydrometeorology, 6*, 330-336

Hamlet, A.F., Mote, P.W., Clark, M.P., & Lettenmaier, D.P. (2005). Effects of temperature and precipitation variability on snowpack trends in the western United States. *Journal of Climate, 18*, 4545-4561

Hansen, J., & Nazarenko, L. (2004). Soot climate forcing via snow and ice albedos. *Proceedings of the National Academy of Sciences, 101*, 423-428

Hansen, J., Sato, M., Ruedy, R., Nazarenko, L., Lacis, A., Schmidt, G.A., Russell, G., Aleinov, I., Bauer, M., Bauer, S., Bell, N., Cairns, B., Canuto, V., Chandler, M., Cheng, Y., Del Genio, A., Faluvegi, G., Fleming, E., Friend, A., Hall, T., Jackman, C., Kelley,

M., Kiang, N., Koch, D., Lean, J., Lerner, J., Lo, K., Menon, S., Miller, R., Minnis, P., Novakov, T., Oinas, V., Perlwitz, J., Rind, D., Romanou, A., Shindell, D., Stone, P., Sun, S., Tausnev, N., Thresher, D., Wielicki, B., Wong, T., Yao, M., & Zhang, S. (2005). Efficacy of climate forcings. *Journal of Geophysical Research-Atmospheres, 110*, doi:10.1029/2005JD005776

IPCC (2007a). Climate Change 2007: A Synthesis Report. In, *The Fourth Assessment of the Intergovernmental Panel on Climate Change.*

IPCC (2007b). Regional Climate Projections. *Climate Change, 2007: The Physical Science Basis. Contribution of Working Group 1 to the Fourth Assessment Report of the Intergovernmental Panel on Climate Change, Chapter 11*, 847-940

Jackson, B.S., & Carroll, J.J. (1978). Aerodynamic roughness as a function of wind direction over asymmetric surface elements. *Boundary-Layer Meteorology, 13*, 7

Kaspari, S., Mayewski, P.A., Handley, M., Kang, S., Hou, S., Sneed, S., Maasch, K., & Qin, D. (2009). A High Resolution Record of Atmospheric Dust Composition and Variability since A.D. 1650 from a Mount Everest Ice Core. *Journal of Climate, 22*, 16

Knowles, N., Dettinger, M.D., & Cayan, D.R. (2006). Trends in snowfall versus rainfall for the western United States. *Journal of Climate, 19*, 14

Lemke, P., Ren, J., Alley, R.B., Allison, I., Carrasco, J., Flato, G., Fujii, Y., Kaser, G., Mote, P.W., Thomas, R.H., & Zhang, T. (2007). *2007: Observations: Changes in Snow, Ice, and Frozen Ground.* . Cambridge, UK & New York, NY, USA: Cambridge University Press

Leung, L.R., Qian, Y., Bian, X., Washington, W.M., Han, J., & Roads, J.O. (2004). Mid-century ensemble regional climate change scenarios for the western United States. *Journal of Climate Change, 62*, 75-113

Liu, J., & Diamond, J. (2005). China's environment in a globalizing world. *Nature, 435*, 1179-1186

Mantua, N.J., Hare, S.R., Zhang, Y.L., Wallace, J.M., & Francis, R.C. (1997). A Pacific interdecadal climate oscillation with impacts on salmon production. *Bulletin of the American Meteorological Society, 78*, 10

Marks, D. (1988). Climate, energy exchange, and snowmelt in Emerald Lake watershed, Sierra Nevada. In, *Department of Geography and Mechanical Engineering* (p. 158). Santa Barbara: University of California

Marks, D., & Dozier, J. (1992). Climate and energy exchange at the snow surface in the alpine region of the Sierra Nevada 2. Snow cover energy balance. *Water Resources Research, 28*, 3043-3054

Marks, D., Dozier, J., & Davis, R.E. (1992). Climate and energy exchange at the snow surface in the alpine region of the Sierra Nevada 1. Meteorological measurements and monitoring. *Water Resources Research, 28*, 3029-3042

Marks, D., Kimball, J., Tingey, D., & Link, T. (1998). The sensitivity of snowmelt processes to climate conditions and forest cover during rain-on-snow: a case study of the 1996 Pacific Northwest flood. *Hydrological Processes, 12*, 24

McConnell, J.R., Aristarain, A.J., Banta, J.R., Edwards, R., & Simoes, J.C. (2007). 20th-Century doubling in dust archived in an Antarctic Peninsula ice core parallels climate change and desertification in South America. *PNAS, 104*, 6

Mote, P.W. (2003). Trends in snow water equivalent in the Pacific Northwest and their climatic causes. *Geophysical Research Letters, 108*, doi:10.1029/2003GL017258

Mote, P.W., Hamlet, A.F., Clark, M.P., & Lettenmaier, D.P. (2005). Declining mountain snowpack in western North America. *Bulletin of the American Meteorological Society, 86*, 39-49

Nash, L.L., & Gleick, P.H. (1991). The sensitivity of streamflow in the Colorado Basin to climatic changes. *Journal of Hydrology, 125*, 221-241

Neff, J., Reynolds, R., Belnap, J., & Lamothe, P. (2005). Multi-decadal impacts of grazing on soil physical and biogeochemical properties in Southeast Utah. *Ecological Applications, 15*, 87-95

Neff, J.C., Ballantyne, A.P., Farmer, G.L., Mahowald, N.M., Conroy, J.L., Landry, C.C., Overpeck, J.T., Painter, T.H., Lawrence, C.R., & Reynolds, R.L. (2008). Increasing eolian dust deposition in the western United States linked to human activity. *Nature Geosciences*

Painter, T.H., Barrett, A.P., Landry, C.C., Neff, J.C., Cassidy, M.P., Lawrence, C.R., McBride, K.E., & Farmer, G.L. (2007). Impact of disturbed desert soils on duration of mountain snow cover. *Geophysical Research Letters, 34*

Painter, T.H., Deems, J., Belnap, J., Hamlet, A.F., Landry, C., & Udall, B. (2010). Response of Colorado River runoff to dust radiative forcing in snow. *PNAS, Submitted*

Pereira, D.C., Evangelista, H., Pereira, E.B., Simoes, J.C., Johnson, E., & Melo, L.R. (2004). Transport of crustal microparticles from Chilean Patagonia to the Antarctic Peninsula by SEM-EDS analysis. *Tellus, 56B*, 14

Pierce, D.W., Barnett, T.P., Hidalgo, H.G., Das, T., Bonfils, C., Santer, B.D., Bala, G., Dettinger, M.D., Cayan, D.R., Mirin, A., Wood, A.W., & Nozawa, T. (2008). Attribution of declining western U.S. snowpack to human effects. *Journal of Climate, 21*, 6425-6444

Pluss, C., & Mazzoni, R. (1994). The role of turbulent heat fluxes in the energy balance of high Alpine snow cover. *Nordic Hydrology, 25*, 13

Poggi, A. (1976). Heat balance in the ablation area of the Ampere Glacier (Kerguelen Islands). *Journal of Applied Meteorology, 16*, 7

Qian, Y., Gustafson, W.I., Leung, L.R., & Ghan, S.J. (2009). Effects of soot-induced snow albedo change on snowpack and hydrological cycle in western United States based on Weather Research and Forecasting chemistry and regional climate simulations. *Journal of Geophysical Research, 114*

Schwikowski, M., Seibert, P., Baltensperger, U., & Gaggeler, H.W. (1995). A study of an outstanding saharan dust event at the high-alpine site Jungfraujoch, Switerland. *Atmospheric Environment, 29*, 1829-1842

Smeets, C.J.P.P., Duynkerke, P.G., & Vugts, H.F. (1999). Turbulence characteristics of the stable boundary layer over a mid-latitude glacier. *Boundary-Layer Meteorology, 92*, 22

Steltzer, H., Landry, C.C., Painter, T.H., Anderson, J., & Ayres, E. (2009). Dust-induced early snowmelt synchronizes phenology across an alpine landscape. *Proceedings of the National Academy of Sciences, 106*, 11629-11634

Stewart, I.T., Cayan, D.R., & Dettinger, M.D. (2004). Changes in snowmelt runoff timing in western North America under a 'business as usual' climate change scenario. *Climatic Change, 62*, 16

Thomas, G., & Rowntree, P.R. (1992). The boreal forests and climate. *Q.J.R Meterological Society, 18*, 28

Thompson, L.G., Yao, T., Mosley-Thompson, E., Davis, M.E., Henderson, K.A., & Lin, P.-N. (2000). A high-resolution millennial record o the south Asian monsoon from Himalayan ice cores. *Science, 289*, 1916-1919

Wake, C.P., & Mayewski, P.A. (1994). Modern eolian dust deposition in central Asia. *Tellus, 46*, 220-233

Waltham, T., & Sholji, I. (2002). The demise of the Aral Sea- an environmental distaster. *Geology Today, 17*, 10

Warren, S.G., & Wiscombe, W.J. (1980). A model for the spectral albedo of snow, II, Snow containing atmospheric aerosols. *Journal of the Atmospheric Sciences, 37*, 2734-2745

Westerling, A.L., Hidalgo, H.G., Cayan, D.R., & Swetnam, T.W. (2006). Warming and Earlier Spring Increase Western US Forest Wildfire Activity. *Science, 313*, 940